EUROPEAN ORGANIZATION FOR NUCLEAR RESEARCH (CERN)

FERMILAB-PUB-16-063-CMS

CERN-PH-EP/2016-008
2016/02/10

CMS-SUS-14-007

Search for supersymmetry in pp collisions at $\sqrt{s} = 8$ TeV in final states with boosted W bosons and b jets using razor variables

The CMS Collaboration*

arXiv:1602.02917v1 [hep-ex] 9 Feb 2016

Abstract

A search for supersymmetry in hadronic final states with highly boosted W bosons and b jets is presented, focusing on compressed scenarios. The search is performed using proton-proton collision data at a center-of-mass energy of 8 TeV, collected by the CMS experiment at the LHC, corresponding to an integrated luminosity of 19.7 fb^{-1}. Events containing candidates for hadronic decays of boosted W bosons are identified using jet substructure techniques, and are analyzed using the razor variables M_{R} and R^2, which characterize a possible signal as a peak on a smoothly falling background. The observed event yields in the signal regions are found to be consistent with the expected contributions from standard model processes, which are predicted using control samples in the data. The results are interpreted in terms of gluino pair production followed by their exclusive decay into top squarks and top quarks. The analysis excludes gluino masses up to 1.1 TeV for light top squarks decaying solely to a charm quark and a neutralino, and up to 700 GeV for heavier top squarks decaying solely to a top quark and a neutralino.

Submitted to Physical Review D

© 2016 CERN for the benefit of the CMS Collaboration. CC-BY-3.0 license

*See Appendix 12 for the list of collaboration members

1 Introduction

The CERN LHC has provided sufficient data to probe a large variety of theories beyond the standard model (SM). Among these, theories based on supersymmetry (SUSY) [1–9], which predict the existence of a spectrum of supersymmetric partners to the SM particles, are strongly motivated. Scenarios with nondegenerate supersymmetric particle spectra, with cross sections as low as ≈1 fb, have been explored in many final states; however, as yet no evidence for SUSY has been found.

The focus of many current searches is so-called natural SUSY [10, 11] in which the Higgs boson mass can be stabilized without excessive fine tuning. In natural SUSY scenarios, the Higgsino mass parameter μ is required to be of the order of 100 GeV, and the lightest top squark $\widetilde{\mathrm{t}}_1$, the gluino $\widetilde{\mathrm{g}}$, and the lightest bottom squark $\widetilde{\mathrm{b}}_1$ are constrained to have masses around the TeV scale, while the masses of the other superpartners are unconstrained and can be much heavier and beyond the LHC reach. The possibility that the top squark could be light has motivated several searches by the ATLAS and CMS collaborations [12–23] for this sparticle. In general, the sensitivity of these searches diminishes for direct top squark production when the mass of the top squark approaches that of the lightest supersymmetric particle (LSP), which is assumed to be the lightest neutralino $\widetilde{\chi}_1^0$. For searches that specifically target the decay $\widetilde{\mathrm{t}}_1 \rightarrow \mathrm{t}\widetilde{\chi}_1^0$, the sensitivity is reduced when the mass difference Δm between the top squark and the LSP is comparable to the top quark mass $m\mathrm{t}$.

Here, we focus on two types of scenarios: the so-called compressed spectrum in which Δm is very small, of order a few GeV to tens of GeV (e.g. [24–26]), and scenarios where $\Delta m \approx m\mathrm{t}$. In the compressed case, the top squark decays to the LSP and soft decay products, which are difficult to detect. When $\Delta m \approx m\mathrm{t}$, the signature of top squark production is very similar to that of $\mathrm{t}\bar{\mathrm{t}}$ production, which has a much higher cross section. Therefore, to be sensitive to such processes, we cannot solely rely on the top squark decay products. Possibilities to discriminate the signal are tagging the top squark events based on a jet from initial state radiation (ISR) using the monojet signature [27, 28], or searching for top squark events in cascade decays of heavier particles, such as the heavy top squark decays $\widetilde{\mathrm{t}}_2 \rightarrow \widetilde{\mathrm{t}}_1 + \mathrm{H/Z}$ [21], or from gluino decays.

In this paper, we search for the challenging top squark final states described above in gluino decays. Specifically, we consider gluino pair production where each gluino decays to a top squark and a top quark. We consider the scenarios in which the gluino has a mass around 1 TeV and the lighter top squark has a mass of a few hundred GeV. Because of the significant mass gap between the gluino and the top squark, the top quark from the gluino decay will receive a large boost. The top squark decays to $\mathrm{c}\widetilde{\chi}_1^0$ for small Δm, or to $\mathrm{t}\widetilde{\chi}_1^0$ for $\Delta m \approx m\mathrm{t}$, as in the targeted searches for $\widetilde{\mathrm{t}}_1 \rightarrow \mathrm{t}\widetilde{\chi}_1^0$ mentioned above. The analysis described in this paper is especially sensitive to the decay $\widetilde{\mathrm{t}}_1 \rightarrow \mathrm{c}\widetilde{\chi}_1^0$. Consequently, this analysis provides new information about the viability of natural SUSY.

The gluino-pair production processes described above, with $\widetilde{\mathrm{t}}_1 \rightarrow \mathrm{c}\widetilde{\chi}_1^0$ or $\widetilde{\mathrm{t}}_1 \rightarrow \mathrm{t}\widetilde{\chi}_1^0$, can be described using simplified model spectra [29–34]. Specifically, the models T1ttcc and T1t1t, shown in Fig. 1, are used in the design of the analysis and in the interpretation of the results.

In light of the discussion above, it is expected that boosted top quarks are a promising signature of new physics involving a massive gluino decaying to a relatively light top squark. Boosted objects with high transverse momentum, p_{T}, are characterized by merged decay products separated by $\Delta R \approx 2m/p_{\mathrm{T}}$, where m denotes the mass of the decaying particle. For the top quark decay products to be merged within the typical jet size of $\Delta R = 0.5$ requires a top quark momentum of ≈700 GeV, a value difficult to reach with proton-proton collisions at 8 TeV.

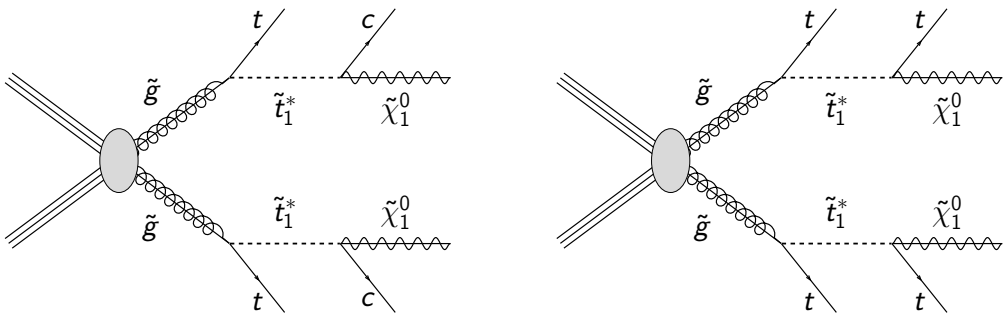

Figure 1: Diagrams for the T1ttcc (left) and T1t1t (right) simplified model spectra. Here, an asterisk (*) denotes an antiparticle of a supersymmetric partner.

Therefore, in order to increase the signal efficiency by entering the boosted regime, we focus on W bosons from top quark decays, which require a more accessible p_{T} around 300 GeV. The targeted final state therefore contains boosted W bosons and jets originating from b quarks (b jets) from top quark decays, light quark jets from unmerged hadronic W boson decay products or charm quarks, and missing energy from the neutralinos. Hadronically decaying boosted W boson candidates are identified using pruned jet mass [35–37] and a jet substructure observable called N-subjettiness [38]. The razor kinematic variables M_{R} and R^2 [39] are used to discriminate the processes with new heavy particles from SM processes in final states with jets and missing transverse energy. To increase the sensitivity to new physics, we perform the analysis by partitioning the (M_{R},R^2) plane into multiple bins.

This paper is organized as follows. The razor variables are introduced in Section 2. Section 3 gives a brief overview of the CMS detector, while Section 4 covers the triggers, data sets, and Monte Carlo (MC) simulated samples used in this analysis. Details of the object definitions and event selection are given in Sections 5 and 6, respectively. Section 7 describes the data/simulation scale factors that are needed to correct the modeling of the boosted W boson tagger. The statistical analysis is explained in Section 8, and Section 9 covers the systematic uncertainties. Finally, our results and their interpretation are presented in Section 10, followed by a summary in Section 11.

2 Razor variables

The razor variables M_{R} and R^2 [39] are useful for describing a signal arising from pair production of heavy particles, each of which decays to a massless visible particle and a massive invisible particle. In the two-dimensional razor plane, a signal with heavy particles is expected to appear as a peak on top of smoothly falling SM backgrounds, which can be empirically described using exponential functions. For this reason, the razor variables are robust discriminators for SUSY signals in which supersymmetric particles are pair-produced and decay to SM particles and the LSP. For the simple case in which the final state comprises two visible particles, e.g. jets, the razor variables are defined using the momenta $\vec{p}^{\,\mathrm{j}_1}$ and $\vec{p}^{\,\mathrm{j}_2}$ of the two jets as

$$M_{\mathrm{R}} \equiv \sqrt{(|\vec{p}^{\,\mathrm{j}_1}| + |\vec{p}^{\,\mathrm{j}_2}|)^2 - (p_z^{\mathrm{j}_1} + p_z^{\mathrm{j}_2})^2}\,, \tag{1}$$

$$M_{\mathrm{T}}^{\mathrm{R}} \equiv \sqrt{\frac{E_{\mathrm{T}}^{\mathrm{miss}}(p_{\mathrm{T}}^{\mathrm{j}_1} + p_{\mathrm{T}}^{\mathrm{j}_2}) - \vec{p}_{\mathrm{T}}^{\mathrm{miss}}\cdot(\vec{p}_{\mathrm{T}}^{\mathrm{j}_1} + \vec{p}_{\mathrm{T}}^{\mathrm{j}_2})}{2}}\,, \tag{2}$$

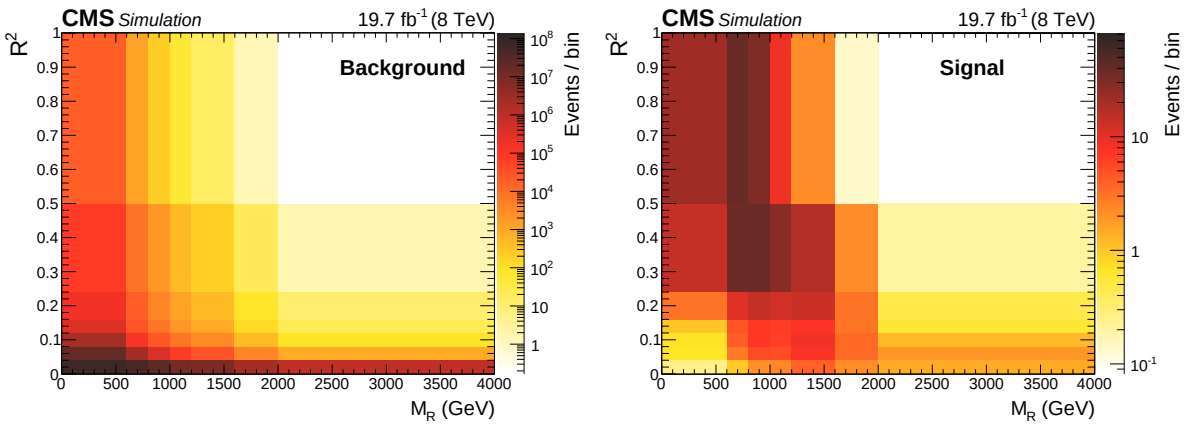

Figure 2: Distributions in the (M_{R},R^2) space of the overall SM backgrounds and a T1ttcc signal with $m_{\tilde{\mathrm{g}}} = 1\,\mathrm{TeV}$, $m_{\tilde{\mathrm{t}}} = 325\,\mathrm{GeV}$ and $m_{\tilde{\chi}_1^0} = 300\,\mathrm{GeV}$, both obtained from simulation. A very loose selection is used: a good primary vertex and at least three jets, one of which is required to have $p_{\mathrm{T}} > 200\,\mathrm{GeV}$.

where $p_z^{\mathrm{j}_{1,2}}$ are the z-components of the $\mathrm{j}_{1,2}$ momenta, $\vec{p}_{\mathrm{T}}^{\,\mathrm{miss}}$ is the missing transverse momentum, computed as the negative vector sum of the transverse momenta of all observed particles in the event, and $E_{\mathrm{T}}^{\mathrm{miss}}$ is its magnitude (see Section 5 for a more precise definition). Given M_{R} and the transverse quantity $M_{\mathrm{T}}^{\mathrm{R}}$, the razor dimensionless ratio is defined as

$$R \equiv \frac{M_{\mathrm{T}}^{\mathrm{R}}}{M_{\mathrm{R}}} \,. \tag{3}$$

If the heavy mother particle is denoted by G and the heavy invisible daughter particle is denoted by χ, the peak of the M_{R} distribution and endpoint of the $M_{\mathrm{T}}^{\mathrm{R}}$ distribution are both estimates of the quantity $(m_{\mathrm{G}}^2 - m_{\chi}^2)/m_{\mathrm{G}}$. When the decay chains are complicated, producing multiple particles in the final state, the razor variables can still be meaningfully calculated by reducing the final state to a two-"megajet" structure. The megajet algorithm aims to cluster visible particles coming from the decays of the same heavy supersymmetric particle. The razor variables M_{R} and R^2 are computed using the four-momenta of the two megajets, where the megajet four-momentum is the sum of the four-momenta of the particles comprising the megajet. Studies show that, of all the possible clusterings, the one that minimizes the sum of the squared invariant masses of the megajets maximizes the efficiency with which particles are matched to their heavy supersymmetric particle ancestor [40].

Figure 2 shows the simulated distributions of the overall SM background and a T1ttcc signal with $m_{\tilde{\mathrm{g}}} = 1\,\mathrm{TeV}$, $m_{\tilde{\mathrm{t}}} = 325\,\mathrm{GeV}$ and $m_{\tilde{\chi}_1^0} = 300\,\mathrm{GeV}$ in the (M_{R},R^2) plane. The SM background, which mainly arises from multijet production, is dominant at low values of R^2, while the SUSY-like signal peaks higher in the (M_{R},R^2) plane (M_{R} peaks around 900 GeV, which is the expected value).

In order to be sensitive to low-$E_{\mathrm{T}}^{\mathrm{miss}}$ scenarios (small Δm), we use a lower R^2 threshold than that used in previous razor analyses [40–43]. To exploit the boosted phase space in which the expected signal significance is greater than in the nonboosted phase space, we work at large $(m_{\mathrm{G}}^2 - m_{\chi}^2)/m_{\mathrm{G}}$ and thus at high M_{R}, allowing us to raise the M_{R} threshold. This has the added virtue of keeping the SM backgrounds at a manageable level.

3 The CMS detector

A detailed description of the CMS detector, together with a definition of the coordinate system used and the relevant kinematic variables, can be found elsewhere [44]. A characteristic feature of the CMS detector is its superconducting solenoid magnet, of 6 m internal diameter, which provides a field of 3.8 T. Within the field volume are a silicon pixel and strip tracker, a lead tungstate crystal electromagnetic calorimeter, and a brass and scintillator hadron calorimeter. Muon detectors based on gas-ionization chambers are embedded in a steel flux-return yoke located outside the solenoid. Events are collected by a two-layer trigger system, where the first level is composed of custom hardware processors, and is followed by a software-based high-level trigger.

The tracking system covers the pseudorapidity region $|\eta| < 2.5$, the muon detector $|\eta| < 2.4$, and the calorimeters $|\eta| < 3.0$. Additionally, the forward region at $3 < |\eta| < 5$ is covered by steel and quartz fibre forward calorimeters. The near hermeticity of the detector permits accurate measurement of the momentum balance in the transverse plane.

4 Trigger and event samples

This analysis is based on a sample of proton-proton collision data at $\sqrt{s} = 8$ TeV collected by the CMS experiment in 2012 and corresponding to an integrated luminosity of 19.7 fb^{-1}. Events are selected using two triggers, requiring either the highest jet p_{T} or the scalar sum H_{T} of jet transverse momenta to be above given thresholds. The jet p_{T} threshold was 320 GeV (and 400 GeV for a brief data taking period corresponding to 1.8 fb^{-1}), while the H_{T} threshold was 650 GeV. The two trigger algorithms were based on a fast implementation of the particle-flow (PF) reconstruction method [45, 46], which is described in Section 5.

To measure the efficiency of these triggers, samples with unbiased jet p_{T} and H_{T} distributions are obtained using an independent set of triggers that require at least one electron or muon. Figure 3 shows, on the left-hand side, the efficiency of the requirement that events satisfy at least one of the two trigger conditions as well as the baseline selection described in Section 6, in the (H_{T}, leading jet p_{T}) plane. The trigger is fully efficient for events with $H_{\text{T}} > 800$ GeV. In order to account for the lower efficiency of the regions with $H_{\text{T}} < 800$ GeV, the measured trigger efficiency over the (H_{T}, leading jet p_{T}) plane is applied as an event-by-event weight to the simulated samples. The right-hand side of Fig. 3 shows the trigger efficiency across the (M_{R}, R^2) plane for the total simulated background.

Simulated event samples are used to investigate the characteristics of the background and signal processes. Multijet, $\text{t}\bar{\text{t}}$, $\text{W}(\to \ell\nu)$+jets, $\text{Z}/\gamma^*(\to \ell\bar{\ell})$+jets, and $\text{Z}(\to \nu\bar{\nu})$+jets events are generated using MADGRAPH 5.1.3.30 [47, 48] with CTEQ6L1 [49] parton distribution functions (PDF), while WW, WZ, and ZZ events are generated using PYTHIA6.424 [50] with CTEQ6L1 PDFs. In what follows, W and Z bosons will be collectively referred to as V. Single top quark events are generated using POWHEG 1.0 [51, 52] and CT10 PDFs [53]. The cross sections for these SM processes are given in Table 2. The inclusive background processes are scaled to the highest-order cross section calculation available, whereas leading-order cross sections are used for $\text{W}(\to \ell\nu)$+jets, $\text{Z}/\gamma^*(\to \ell\bar{\ell})$+jets, and $\text{Z}(\to \nu\bar{\nu})$+jets, which are produced with varying generator-level H_{T} requirements. The simplified model signals are produced using MADGRAPH 5.1.5.4 using CTEQ6L1 PDFs. The signal cross sections are computed at next-to-leading order with next-to-leading-log corrections using PROSPINO and NLL-FAST [54–59]. The parton-level events are showered and hadronized using PYTHIA6.426 with tune Z2* [60], which is derived from the Z1 tune [61]. The latter uses the CTEQ5L PDFs [62], whereas Z2* adopts

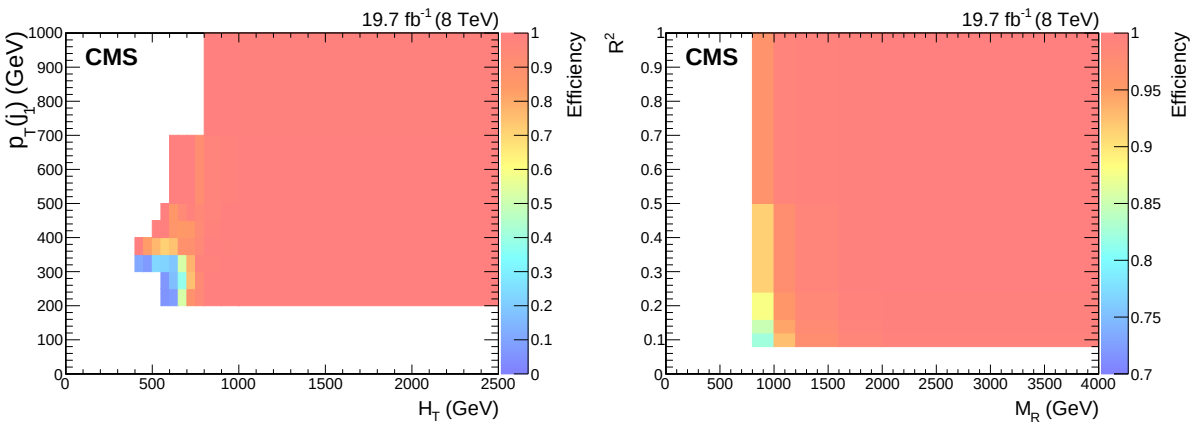

Figure 3: (Left) The trigger efficiency, obtained from data, as a function of H_T and leading jet p_T after the baseline selection discussed in Section 6. (Right) The trigger efficiency as a function of M_R and R^2 after the same baseline selection, obtained by applying the trigger efficiency as a function of H_T and leading jet p_T to the simulated background.

CTEQ6L. For the background events, the response of the CMS detector is simulated in detail using a program (FULLSIM) based on GEANT4 [63]. A parameterized fast detector simulation program (FASTSIM) is used to simulate the detector response for the signal events [64].

5 Event reconstruction

We select events that have at least one interaction vertex associated with at least four charged-particle tracks. The vertex position is required to lie within 24 cm of the center of the CMS detector along the beam direction and within 2 cm from the center in the plane transverse to the beam. Because of the high instantaneous luminosity of the LHC, hard scattering events are typically accompanied by overlapping events from multiple proton-proton interactions (pileup), and therefore contain multiple vertices. We identify the primary vertex, i.e., the vertex of the hard scatter, as the one with the highest value of the $\sum p_T^2$ of the associated tracks. Detector- and beam-related filters are used to discard events with anomalous noise that mimic events with high energy and large imbalance in transverse momentum [65, 66].

CMS reconstructs events using the PF algorithm, in which candidate particles (PF candidates) are formed by combining information from the inner tracker, the calorimeters, and the muon system. Each PF candidate is assigned to one of five object categories: muons, electrons, photons, charged hadrons, and neutral hadrons. Contamination from pileup events is reduced by discarding charged PF candidates that are incompatible with having originated from the primary vertex [67]. The average pileup energy associated with neutral hadrons is computed event-by-event and subtracted from the jet energy and from the energy used when computing lepton isolation, i.e., a measure of the activity around the lepton. The energy subtracted is the average pileup energy per unit area (in $\Delta\eta \times \Delta\phi$) times the jet or isolation cone area [68, 69].

Jets are clustered with FASTJET 3.0.1 [70] using the anti-k_T algorithm [71] with distance parameter $\Delta R = 0.5$. These jets are referred to as AK5 jets. Corrections are applied as a function of jet p_T and η to account for the residual effects of nonuniform detector response. The jet energies are corrected so that, on average, they match those of simulated particle-level jets [72]. After correction, jets are required to have $p_T > 30$ GeV and $|\eta| < 2.4$. We use the combined secondary vertex algorithm [73, 74] to identify jets arising from b quarks. The medium tagging criterion, which yields a misidentification rate for light quark and gluon jets of ≈1% and a typical effi-

ciency of ≈70%, is used to select b jets. The loose tagging criterion, with a misidentification rate of ≈10% and efficiency of ≈85%, is used to reject events containing b jets.

To identify boosted W bosons, we follow a similar procedure as outlined in Ref. [75]. Jets are clustered with FASTJET using the Cambridge-Aachen algorithm [76] and a distance parameter of 0.8, yielding CA8 jets. Jet energy corrections for these jets are derived from the anti-k_T jets with distance parameter $\Delta R = 0.7$. Simulations show that the corrections are valid for CA8 jets and have an additional uncertainty $\leq 2\%$.

The jet mass is calculated from the constituents of the jet after jet pruning, which removes the softest constituents of the jet. During jet pruning, the jet constituents are reclustered, and at each step the softer and larger-angle "protojet" of the two protojets to be merged is removed should it fail certain criteria [35, 36]. A CMS study has shown that jet pruning reduces pileup effects and provides good discrimination between boosted W jets and quark/gluon (q/g) jets [37]. We define mass-tagged jets (mW) as CA8 jets with $p_T > 200\,\text{GeV}$ and jet mass within the range $70 < m_{\text{jet}} < 100\,\text{GeV}$ around the W boson mass.

In addition to the jet mass, we also consider the N-subjettiness [38] variables, which are obtained by first finding N candidate axes for subjets in a given CA8 jet, and then computing the quantity

$$\tau_N = \frac{1}{R_0} \sum_k p_{T,k} \min(\Delta R_{1,k}, \Delta R_{2,k}, ...\Delta R_{N,k}) / \sum_k p_{T,k}, \tag{4}$$

where R_0 is the original jet distance parameter and k runs over all constituent particles. The subjet axes are obtained with FASTJET via exclusive k_T clustering, followed by a one-pass optimization to minimize the N-subjettiness value. The quantity τ_N is small if the original jet is consistent with having N or fewer subjets. Therefore, to discriminate boosted W bosons, which have two subjets, from q/g jets characterized by a single subjet, we require that a W boson mass-tagged jet satisfy $\tau_2/\tau_1 < 0.5$ for it to be classified as a W boson tagged jet (labeled W in the following). The W boson tagging efficiency is dependent on the CA8 jet p_T, and is 50–55% according to simulation. The corresponding misidentification rate is 3–5%. We also define W boson anti-tagged jets (aW) as W boson mass-tagged jets that satisfy the complement of the τ_2/τ_1 criterion, and use these jets to define control regions for data-driven background modeling.

To calculate $\vec{p}_T^{\text{miss}}$, which is used in the calculation of the razor variable R^2 defined in Eqs. (2) and (3), the vector sum over the transverse momenta is taken of all the PF candidates in an event.

Loosely identified and isolated electrons [77] (and muons [78]) with $p_T > 5\,\text{GeV}$ and $|\eta| < 2.5$ (2.4) are used both to suppress backgrounds in the signal region and in the definition of the control regions. Tightly identified isolated leptons, electrons (muons) with $p_T > 10\,\text{GeV}$ and $|\eta| < 2.5$ (2.4), define a control region enriched in $Z \to \ell\bar{\ell}$ events, from which we estimate the systematic uncertainty in the predicted number of $Z \to \nu\bar{\nu}$ events in the signal region. Electron candidates that lie in the less well-instrumented transition region between the barrel and endcap calorimeters, $1.44 < |\eta| < 1.57$, are rejected. We suppress background from events that are likely to contain τ and other leptons that fail the loose selection by discarding events with isolated tracks with $p_T > 10\,\text{GeV}$ and track-primary vertex distance along the beam direction $|d_z| < 0.05\,\text{cm}$.

Known differences between the properties of data and MC simulated data are corrected by weighting simulated events with data/simulation scale factors for the jet energy scale, b tag, W mass-tag, W tag and W anti-tag efficiency. The W tagging-related scale factors are described

in Section 7. In addition, event-by-event weights are used to correct the simulated data so that their pileup, trigger, top quark p_{T}, and ISR characteristics match those of data.

6 Analysis strategy and event selection

We search for deviations from the SM in the (high-M_{R}, high-R^2) region using events with at least one boosted W boson, at least one b-tagged jet and no isolated leptons or tracks. SM backgrounds in the signal region S are estimated using observations in control regions and scale factors, calculated from MC simulation, that relate the number of events in one region to that in another. Three control regions, Q, T, and W, select high-purity samples of multijet, $\mathrm{t\bar{t}}$, and $\mathrm{W}(\to \ell\nu)$+jets events, respectively. Details of the background estimation method are given in Section 8.

Events must satisfy the following baseline selection:

1. have at least one good primary vertex (see Section 5);
2. pass all detector- and beam-related filters (see Section 5);
3. have at least three selected AK5 jets of which at least one has $p_{\mathrm{T}} > 200\,\mathrm{GeV}$, thereby defining the boosted phase space; and
4. satisfy $M_{\mathrm{R}} > 800\,\mathrm{GeV}$ and $R^2 > 0.08$, where the megajets are constructed from the selected AK5 jets.

The details of the event selection in addition to the baseline selection are given in Table 1. The signal and control regions are defined using different requirements on the multiplicities of leptons, b-tagged jets and W-tagged jets, and on kinematic variables that discriminate between different processes. The multijet-enriched control sample Q is used for estimating the multijet background in the S and T regions. To characterize Q, we use the fact that $E_{\mathrm{T}}^{\mathrm{miss}}$ in multijet events is largely due to jet mismeasurements rather than the escape of particles that interact weakly with the detector; consequently, $\vec{p}_{\mathrm{T}}^{\mathrm{miss}}$ will often be aligned with one of the jets. Therefore, a good discriminant between multijet events and events with genuine $E_{\mathrm{T}}^{\mathrm{miss}}$ is

$$\Delta\phi_{\mathrm{min}} = \min_i \Delta\phi(\vec{p}_{\mathrm{T}}^{\mathrm{miss}}, \vec{p}_{\mathrm{T}\,i}), \tag{5}$$

that is, the minimum of the angles between $\vec{p}_{\mathrm{T}}^{\mathrm{miss}}$ and the transverse momentum of each jet, where i runs over the three leading AK5 jets.

The T and W control regions are used to characterize the $\mathrm{t\bar{t}}$ and W+jets backgrounds, respectively, in the S region. The contamination in the S region from fully hadronic decays of $\mathrm{t\bar{t}}$ pairs is negligible because they do not produce sufficient genuine $E_{\mathrm{T}}^{\mathrm{miss}}$ to satisfy our event selection. The $\mathrm{t\bar{t}}$ contamination consists thus of the semileptonic decays of $\mathrm{t\bar{t}}$ pairs in which one W boson is boosted and the other W boson decays to a charged lepton that is not identified. Therefore, the T region is required to have a lepton from the decay of a W boson, at least one b-tagged jet, and a W-tagged jet. Similarly, the W+jets contribution in the S region comes from leptonic W boson decays in which the charged lepton is not identified and a jet is misidentified as a W jet. Therefore, we require the W region to have events with a lepton from the W boson and a mass-tagged boosted W jet, which is a quark or gluon initiated jet misidentified as a boosted W boson. The N-subjettiness criterion is not imposed in order to maintain high event yields in these control regions and therefore higher statistical precision.

Table 1: Summary of the selections used, in addition to the baseline selection, to define the signal region (S), the three control regions (Q, T, W), and the two regions (S', Q') used for the cross-checks described later in the text.

Selection	S	S'	Q	Q'	T	W
Number of b-tagged jets	$\geq$1	$\geq$1	0	0	$\geq$1	0
Number of mass-tagged Ws	$\geq$1	$\geq$1	$\geq$1	$\geq$1	$\geq$1	$\geq$1
Number of tagged Ws	$\geq$1	$\geq$1	—	—	$\geq$1	—
Number of anti-tagged Ws	—	—	$\geq$1	$\geq$1	—	—
Number of loose leptons	0	0	0	0	1	1
Number of isolated tracks	0	0	0	0	—	—
m_{T} (GeV)	—	—	—	—	$<$100	30–100
$\Delta\phi_{\mathrm{min}}$	$>$0.5	$<$0.5	$<$0.3	$>$0.5	$>$0.5	$>$0.5

In the T and W regions, we suppress potential signals using the transverse mass,

$$m_{\mathrm{T}} = \sqrt{2 p_{\mathrm{T}}^{\ell} E_{\mathrm{T}}^{\mathrm{miss}} (1 - \cos\Delta\phi)}, \tag{6}$$

where $\Delta\phi$ is the difference in azimuthal angle between the lepton $\vec{p}_{\mathrm{T}}$ and $\vec{p}_{\mathrm{T}}^{\mathrm{miss}}$, and p_{T}^{ℓ} is the magnitude of the lepton $\vec{p}_{\mathrm{T}}$. The m_{T} distribution exhibits a kinematic edge at the mass of the W boson for $\mathrm{t\bar{t}}$ and $\mathrm{W}(\rightarrow\ell\nu)$+jets processes. However, such an edge is not present for signal events because of the extra contribution to $E_{\mathrm{T}}^{\mathrm{miss}}$ from neutralinos, which escape direct detection. Therefore, potential signals are suppressed in the T and W regions by requiring $m_{\mathrm{T}} < 100\,\mathrm{GeV}$. For the W region, we additionally require $m_{\mathrm{T}} > 30\,\mathrm{GeV}$ in order to reduce residual contamination from multijet events, which are expected to have small $E_{\mathrm{T}}^{\mathrm{miss}}$ and therefore small m_{T}. Table 1 lists two additional control regions, S' and Q', which are used in the cross-checks described later in this section.

Figure 4 shows the simulated distributions in the signal region for the M_{R} and R^2 variables, where the smoothly falling nature of the backgrounds, as well as their relative contributions, can be observed. The m_{T} distribution in the T and W regions prior to the m_{T} and $\Delta\phi_{\mathrm{min}}$ selection is shown in Fig. 5, while Fig. 6 shows the $\Delta\phi_{\mathrm{min}}$ distribution in the Q region, both for data and simulated backgrounds. Overall, there is reasonable agreement between the observed and simulated yields. The discrepancies are accommodated by the systematic uncertainties we assign to the simulated yields.

In Table 2, we show the expected number of events obtained from simulation for the different background processes and for the example T1ttcc model with $m_{\tilde{\mathrm{g}}} = 1\,\mathrm{TeV}$, $m_{\tilde{\mathrm{t}}} = 325\,\mathrm{GeV}$ and $m_{\tilde{\chi}_1^0} = 300\,\mathrm{GeV}$. The observed event counts after different levels of selection, beyond the trigger requirement, are also reported. The background composition in percent after the baseline, S, Q, T, and W region selections is reported in Table 3. The signal region is $\mathrm{t\bar{t}}$ dominated, with additional contributions from $\mathrm{W}(\rightarrow\ell\nu)$+jets and multijet processes. Each control region, Q, T, and W, has high purity for the background process it targets, 90% multijet, 83% $\mathrm{t\bar{t}}$ and single top quark processes, and 85% $\mathrm{W}(\rightarrow\ell\nu)$+jets, respectively. The discrepancies between the observations and the simulation are due to uncertainties in the MC modeling, especially for the multijet processes.

We do not explicitly estimate the background in the signal region. Rather, from the observations in the control regions, we create a prior distribution (described in Section 8) for the four background components of the signal region that incorporates all statistical and systematic uncertainties. However, in order to verify that the control regions in data provide adequate models for backgrounds in the signal region and that the translations between different regions

Table 2: Event yields in simulated event samples and in data as event selection requirements are applied. The simulated event counts are normalized to an integrated luminosity of 19.7 fb^{-1}. "Other" refers to the sum of the small background components $Z/\gamma^* \to \ell\bar{\ell}$+jets, triboson, and $t\bar{t}V$. The signal is the T1ttcc model with $m_{\tilde{g}} = 1000\,\mathrm{GeV}$, $m_{\tilde{t}_1} = 325\,\mathrm{GeV}$, $m_{\tilde{\chi}_1^0} = 300\,\mathrm{GeV}$. The row corresponding to "$n_{\mathrm{PV}} > 0$" gives the event counts after applying the noise filters, pileup reweighting, top p_{T} reweighting for $t\bar{t}$, ISR reweighting for the signal, and the requirement of at least one primary vertex. The column listing the total number of background events also includes some processes that only contribute at the early stages of the event selection. The cross sections used for each sample are listed in the second line of the header. Several of the simulated background samples were produced with generator-level selections applied, which are not fully covered by the first selection levels listed in this table.

Selection	Multijet 10.4×10^7 pb	$t\bar{t}$ 245.8 pb	$W(\to \ell\nu)$ 111.5 pb	Diboson 95.4 pb	Single top 114.9 pb	$Z(\to \nu\bar{\nu})$ 588.3 pb	Other 25.2 pb	Total background	Signal 0.02435 pb	Data
No selection	2.1×10^{11}	4.9×10^6	2.2×10^6	1.9×10^6	2.3×10^6	1.2×10^7	4.9×10^5	2.1×10^{11}	499	
$n_{\mathrm{PV}} > 0$	1.05×10^{11}	4.42×10^6	2.02×10^6	1.08×10^6	1.72×10^6	2.87×10^6	4.0×10^5	1.05×10^{11}	479	
$n_{\mathrm{j}} \geq 3$	2.04×10^{10}	4.08×10^6	1.51×10^6	5.19×10^5	1.10×10^6	6.24×10^5	3.37×10^5	2.05×10^{10}	472	
$p_{\mathrm{T}}(\mathrm{j}_1) > 200\,\mathrm{GeV}$	1.82×10^8	2.88×10^5	4.36×10^5	1.86×10^4	6.08×10^4	5.89×10^4	7.23×10^4	1.82×10^8	403	
$M_{\mathrm{R}} > 800, R^2 > 0.08$	3.47×10^4	5.83×10^3	1.17×10^4	309	900	3.25×10^3	645	57 557	224	
Trigger	3.15×10^4	5.12×10^3	9.38×10^3	249	786	2.32×10^3	569	50 164	216	67 037
No leptons	3.09×10^4	1.87×10^3	3.75×10^3	96.3	311	2.30×10^3	216	39 666	142	56 220
$n\mathrm{b} \geq 1$	9.37×10^3	1.51×10^3	590	25.2	226	302	79.8	12 187	119	18 164
$n\mathrm{W} \geq 1$	841	332	56.4	8.52	56.7	22.1	16.9	1 350	28	1 817
S	14.8	90.4	23.1	3.7	11.7	12.7	4.17	160	23.4	187
$n\mathrm{b} = 0$	1.25×10^4	98.3	1.70×10^3	35.6	25.9	1.25×10^3	54.3	15 691	5.65	20 667
$n_{\mathrm{aW}} \geq 1$	1519	18.7	204	8.36	7.40	158	6.98	1 923	0.667	2 712
Q	1447	10.6	93.1	3.88	3.94	38.9	4.48	1 603	0.07	2 240
1 lepton	585.9	2.74×10^3	5.52×10^3	132	421	22.1	272	9 699	65.0	10 008
$n\mathrm{b} \geq 1$	236.7	2.17×10^3	625	29.9	301	4.14	102	3 470	54	3 930
$n\mathrm{W} \geq 1$	24.3	496	61.6	10.0	50.9	0.56	21.9	666	12.3	770
T	0	112	20.2	2.0	13.3	0	4.1	151	1.2	153
$n\mathrm{b} = 0$	150.5	153	2.86×10^3	52.8	41.3	11.5	68.8	3 329	2.54	3 165
$n_{mW} \geq 1$	30.8	79.1	605	33.1	13.8	2.4	20.3	786	1.19	581
W	0	15.5	127	3.6	1.6	0.64	1.4	150	0.06	116

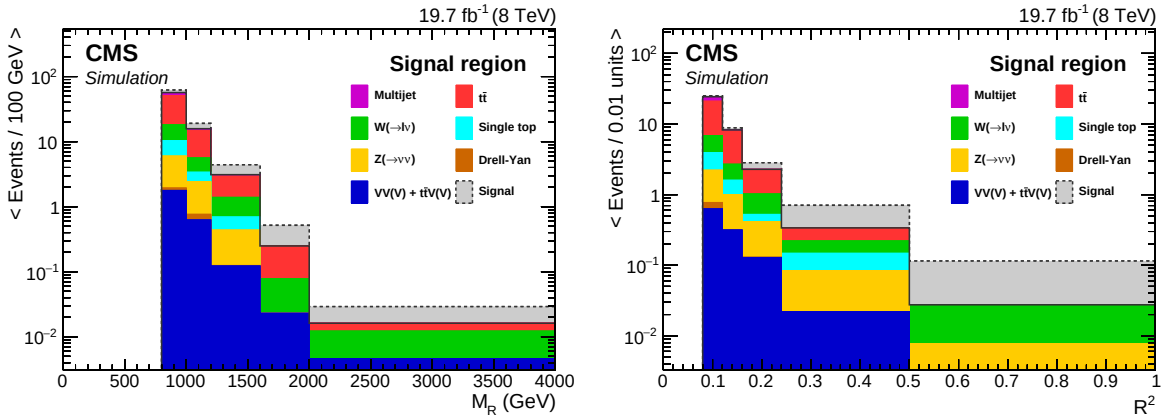

Figure 4: Simulated M_{R} (left) and R^2 (right) distributions in the signal region, S. Stacked on top of the background distributions is the predicted signal contribution from an example T1ttcc model, with parameters $m_{\tilde{\mathrm{g}}} = 1\,\mathrm{TeV}$, $m_{\tilde{\mathrm{t}}} = 325\,\mathrm{GeV}$ and $m_{\tilde{\chi}_1^0} = 300\,\mathrm{GeV}$. The bin entries are normalized proportionally to the bin width.

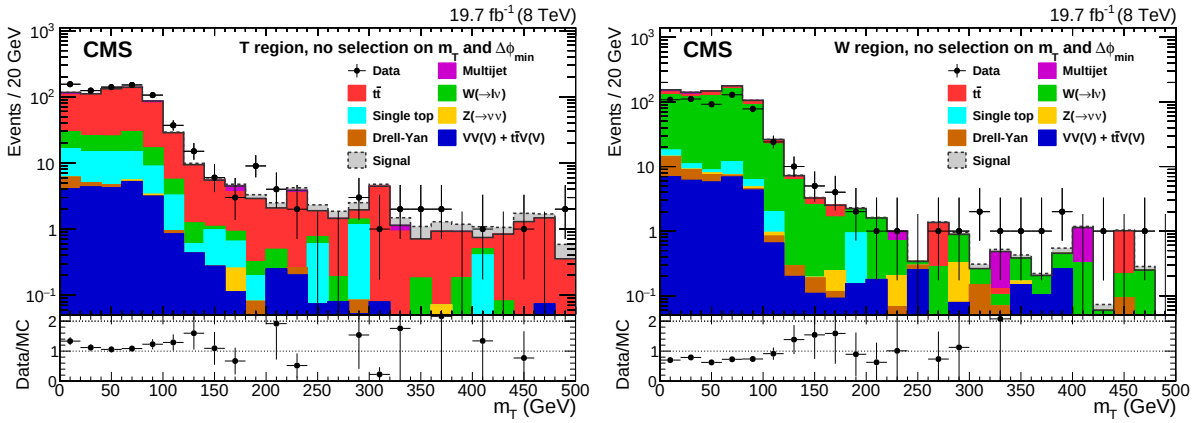

Figure 5: Distributions of m_{T} for data and simulated backgrounds, in the T (left) and W (right) control regions, without applying any selection on m_{T} and $\Delta\phi_{\mathrm{min}}$. The contribution from an example signal corresponding to the T1ttcc model with $m_{\tilde{\mathrm{g}}} = 1\,\mathrm{TeV}$, $m_{\tilde{\mathrm{t}}} = 325\,\mathrm{GeV}$ and $m_{\tilde{\chi}_1^0} = 300\,\mathrm{GeV}$, is stacked on top of the background processes. Only statistical uncertainties are shown.

behave as expected, we perform two cross-checks, taking into account statistical uncertainties only.

In the first cross-check, we predict the background in a signal-like control region, and compare these predictions with the observations in that region. This control region, denoted by S', is defined by inverting the $\Delta\phi_{\mathrm{min}}$ requirement while preserving the rest of the signal selection. The estimated number of events in the S' region for the multijet, $\mathrm{W}(\to \ell\nu)$+jets, and top quark processes is computed as follows,

$$\widehat{N}^{S'}_{\mathrm{QCD}} = \left(N^{Q}_{\mathrm{obs}} - N^{Q}_{\mathrm{other,MC}}\right) / \left(\frac{N^{Q}_{\mathrm{QCD}}}{N^{S'}_{\mathrm{QCD}}}\right)_{\mathrm{MC}}, \tag{7}$$

$$\widehat{N}^{S'}_{\mathrm{W}(\to\ell\nu)} = \left(N^{W}_{\mathrm{obs}} - N^{W}_{\mathrm{other,MC}}\right) / \left(\frac{N^{W}_{\mathrm{W}(\to\ell\nu)}}{N^{S'}_{\mathrm{W}(\to\ell\nu)}}\right)_{\mathrm{MC}}, \tag{8}$$

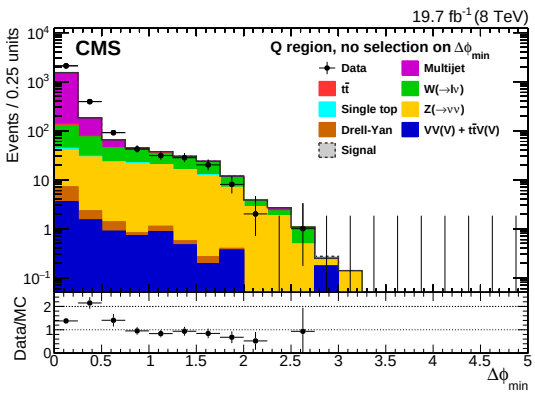

Figure 6: Distributions of $\Delta\phi_{\text{min}}$ for data and simulated backgrounds in the Q region without applying a selection on $\Delta\phi_{\text{min}}$. Only statistical uncertainties are shown. Signal contamination in this control region is negligible.

Table 3: Background composition according to simulation after the baseline, S, Q, T, W, Q' and S' region selections. "Other" refers to the sum of the small background components $Z/\gamma^* \to \ell\bar{\ell}$, triboson, and $t\bar{t}V$.

Selection	Multijet (%)	$t\bar{t}$ (%)	$W(\to \ell\nu)$ (%)	Diboson (%)	Single top (%)	$Z(\to \nu\bar{\nu})$ (%)	Other (%)
Baseline	62.8	10.2	18.7	0.5	1.6	4.6	1.6
S	9.2	56.3	14.4	2.3	7.3	7.9	2.6
Q	90.2	0.7	5.8	0.2	0.2	2.4	0.3
T	0.0	73.9	13.3	1.3	8.8	0.0	2.7
W	0.0	10.3	84.8	2.4	1.1	0.4	1.0
Q'	12.3	2.8	36.8	1.7	1.0	45.0	0.4
S'	69.5	20.3	2.8	0.4	3.8	0.8	2.4

$$\widehat{N}^{S'}_{\text{TTJ+T}} = \left(N^{T}_{\text{obs}} - \widehat{N}^{T}_{\text{QCD}} - N^{T}_{\text{other,MC}}\right) / \left(\frac{N^{T}_{\text{TTJ+T}}}{N^{S'}_{\text{TTJ+T}}}\right)_{\text{MC}}, \tag{9}$$

while the estimated number of multijet events in the control region T is given by

$$\widehat{N}^{T}_{\text{QCD}} = \left(N^{Q}_{\text{obs}} - N^{Q}_{\text{other,MC}}\right) / \left(\frac{N^{Q}_{\text{QCD}}}{N^{T}_{\text{QCD}}}\right)_{\text{MC}}. \tag{10}$$

In Eqs. (7)–(10), the superscripts denote one of the control regions, while the subscripts "other", "$W(\to \ell\nu)$", "TTJ + T", and "QCD", denote the sum of the small backgrounds, $W(\to \ell\nu)$+jets, $t\bar{t}$ plus single top quark, and multijet, respectively, while "obs" labels observed counts. These equations are used only in this cross-check. However, they incorporate the same relations between signal and control regions as will be used in the likelihood procedure described in Section 8. As can be seen from Table 3, the nominal choice of the parameters associated with systematic uncertainties leads to $N^{T}_{\text{QCD,MC}} = 0$. The total estimated background in S' is

$$\widehat{N}^{S'} = \sum_{i} \widehat{N}^{S'}_{i}, \tag{11}$$

where i runs over all background processes. For smaller backgrounds, $\widehat{N}^{S'}_{i}$ is determined by simulation. Backgrounds are estimated bin-by-bin in the (M_{R}, R^2) space, where the bin boundaries are numerically defined in Table 5. However, the estimated scale factors are global as the

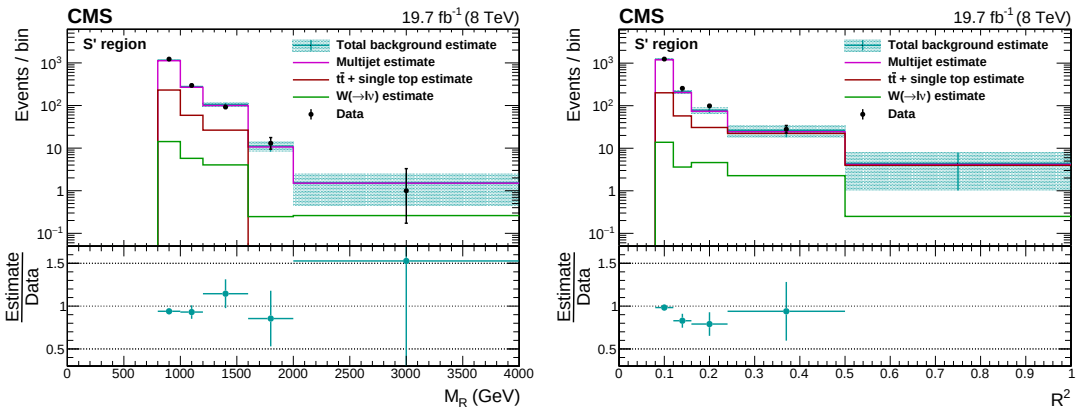

Figure 7: One-dimensional projection of M_R (left) and R^2 (right) for the cross-check predicting the $\Delta\phi_{\text{min}}$ sideband region S'. The estimates for the three different background processes are stacked on top of each other. The uncertainties shown are statistical only. The horizontal error bars indicate the bin width.

statistical precision is not sufficient to yield reliable bin-by-bin estimates. The expected global scale factors, which we denote by κ, are defined in Section 8, which also describes how they are calculated.

Figure 7 shows the projection on the M_R and R^2 axes of the predicted and observed distributions in the S' region. The prediction agrees with observation within ≈20%. This cross-check of the background modeling shows that it is feasible to estimate a multicomponent background in a signal-like region using the control regions we have defined.

In the second cross-check, we use the Q region to estimate the background in a signal-like Q region, denoted by Q', for which $\Delta\phi_{\text{min}} > 0.5$, from the relationship

$$\widehat{N}^{Q'} = N^{Q}_{\text{obs}} \frac{N^{Q'}_{\text{MC}}}{N^{Q}_{\text{MC}}}. \tag{12}$$

Here N_{MC} includes all contributing background processes, and N^{Q}_{obs} is the observed count in the Q region. This test assesses the degree to which the simulated distribution of $\Delta\phi_{\text{min}}$ as well as its extrapolation from the Q region to the S region are reliable. As observed from Table 3, the multijet process is only a small contribution in the Q' region. Therefore, this cross-check assesses how well the reduction of the multijet process, via the $\Delta\phi_{\text{min}} > 0.5$ requirement, is modeled. The comparison between prediction and observation can be made from data shown in Fig. 8. The level of discrepancy between the prediction and observation in this cross-check is incorporated as a systematic uncertainty of 42% in the global scale factor for the multijet component, as described in Section 8.

7 The W boson tagging scale factors

The W boson tagger used in this analysis is the same as that defined and used in previous CMS analyses [75, 79]. Since the W boson tagging efficiency does not depend significantly on the event topology, we use the same scale factor [75]

$$\text{SF}_{\text{Wtag}} = 0.86 \pm 0.07, \tag{13}$$

as used in these previous analyses, for correcting the modeling differences between FULLSIM and data for the W boson tagging efficiency and apply the scale factor to processes with genuine

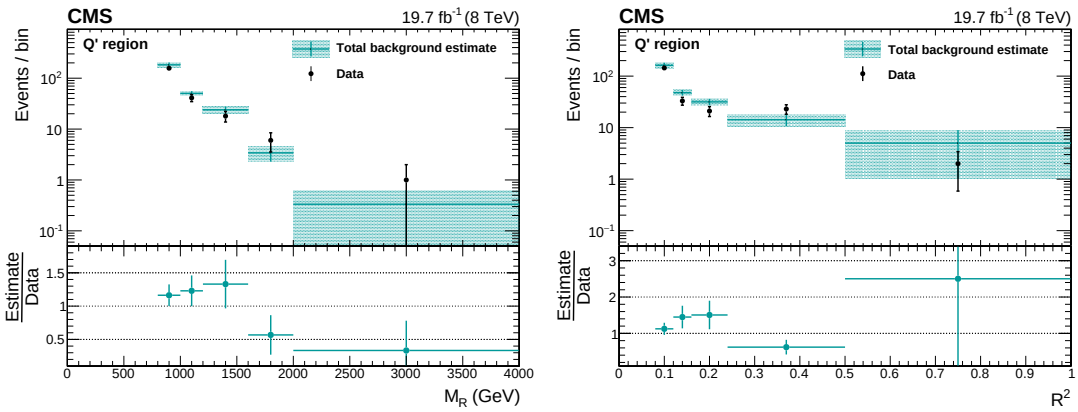

Figure 8: One-dimensional projection of M_R (left) and R^2 (right) for the cross-check predicting the background in region Q' defined by $\Delta\phi_{\text{min}} > 0.5$. The uncertainties shown are statistical only. The horizontal error bars indicate the bin width.

hadronically decaying W bosons (mainly $t\bar{t}$ and signal) in the S and T regions.

On the other hand, the data/FULLSIM scale factors for the misidentification (mistag) efficiency for mass-tagged, anti-tagged, and tagged W bosons are derived specifically for this analysis. The mistag efficiency is defined as the probability to tag, with one of the W taggers, a jet not originating from the hadronic decay of a W boson. Scale factors are necessary to correct the mistag efficiencies for W boson mass-tagging and anti-tagging in the MC simulation of the Q and W control regions, respectively, whereas the mistag efficiency scale factor for W boson tagging is used to correct simulated events with misidentified W bosons, e.g. multijet or $W(\to \ell\nu)$+jets events, in the S and T regions. All three mistag efficiency scale factors are derived using the same multijet-enriched control region, defined as region Q with the exception of all selection related to razor variables and W tagging. To obtain the mistag efficiencies ϵ_f for W boson tagging, mass-tagging and anti-tagging, we use the leading CA8 jet in each event and measure the fraction of these jets passing the given tagger. After obtaining ϵ_f in both data and FULLSIM, we compute the scale factor,

$$\text{SF}(p_T) = \frac{\epsilon_f^{\text{data}}(p_T)}{\epsilon_f^{\text{FULLSIM}}(p_T)}. \tag{14}$$

The scale factors for the W boson tagging, mass-tagging and anti-tagging mistag efficiency vary between 1.0–1.2, 1.1–1.4, and 1.2–1.5, respectively, depending on the CA8 jet p_T. The uncertainties in the scale factor include the statistical uncertainty as well as the trigger efficiency and jet energy scale uncertainties, and vary between 2–7% depending on the CA8 jet p_T.

Because the signal processes are simulated with FASTSIM, the resulting tagging efficiencies must be corrected for modeling differences between the programs FASTSIM and FULLSIM. To compute the W boson tagging efficiency FULLSIM/FASTSIM scale factor we use a sample of $t\bar{t}$ events simulated with FULLSIM and FASTSIM. We first determine the W boson tagging efficiency for both samples, considering only events with exactly one hadronically decaying W boson at the generator level for which the closest reconstructed CA8 jet lies within $\Delta R = 0.8$ of the W boson. Since we wish to select boosted W bosons, and not boosted top quarks, we require that there be no (generator-level) b quark from the top quark decay within the cone of the closest CA8 jet. The W boson tagging efficiency as a function of p_T for a given sample is then obtained by dividing the p_T distribution of the closest CA8 jets that also satisfy the tagging condition ($70 < m_{\text{jet}} < 100\,\text{GeV}$ and $\tau_2/\tau_1 < 0.5$) by the p_T distribution of all closest CA8 jets. To determine the FULLSIM/FASTSIM scale factor for the W boson tagging efficiency,

we divide the efficiencies ϵ obtained from the FULLSIM and FASTSIM samples, $\mathrm{SF}_{\mathrm{Full/Fast}}(p_{\mathrm{T}}) = \epsilon^{\mathrm{FULLSIM}}(p_{\mathrm{T}})/\epsilon^{\mathrm{FASTSIM}}(p_{\mathrm{T}})$. This scale factor is applied to all signal samples and varies between 0.89–0.95, depending on the p_{T} of the given CA8 jet, with an uncertainty of less than 3%.

8 Statistical analysis

The statistical analysis of the observations in the signal region is based on a likelihood function, $L(\sigma)$, given by

$$L(\sigma) = \int \mathrm{d}\mathcal{L} \int \mathrm{d}\vec{\theta}_1 \cdots \int \mathrm{d}\vec{\theta}_M \left[\prod_{i=1}^{M} p(N_i^S|\sigma, \mathcal{L}, \vec{\theta}_i) \right] \pi(\vec{\theta}_1, \cdots, \vec{\theta}_M)\, \pi(\mathcal{L}), \tag{15}$$

where σ is the total signal cross section, $M = 25$ is the number of bins in the (M_{R}, R^2) plane, N_i^S is the observed count in bin i of the signal region, and the bin-by-bin parameters ϵ, b^S_{QCD}, b^S_{TTJ}, $b^S_{\mathrm{W}(\to\ell\nu)}$, and b^S_{other} are denoted collectively by $\vec{\theta}$. The parameter ϵ represents the M signal efficiencies (including acceptance) for a given signal model, while the bin-by-bin background parameters for a given background process in the S region are denoted by b^S_{process}. The function $\pi(\mathcal{L})$ is the integrated luminosity prior and $\pi(\vec{\theta}_1, \cdots, \vec{\theta}_M)$ is an evidence-based prior constructed from observations in the control regions and the four global scale factors $\kappa^{A/B}_{\mathrm{process}} = \sum_i b^A_{\mathrm{process,MC},i} / \sum_i b^B_{\mathrm{process,MC},i}$, where the sum is over all bins of the simulated data; A and B denote any of the S, Q, T, or W regions.

The association of the global scale factors with the control regions is shown in Fig. 9, which also shows which control regions provide constraints on the background parameters, b^S_{process}. Although we use the same global scale factors in each bin, shape uncertainties in the simulated distributions are accounted for by allowing the uncertainty in the scale factors to be bin-dependent. The 25 signal bins in the (M_{R}, R^2) plane are divided into three sets for which different uncertainties are applied: the four bins nearest the origin (set 1), the five surrounding bins (set 2), and the remaining bins (set 3). The likelihood per bin is taken to be $p(N^S|\sigma, \mathcal{L}, \vec{\theta}) = \mathrm{Poisson}(N^S, \epsilon\sigma\mathcal{L} + b^S_{\mathrm{QCD}} + b^S_{\mathrm{TTJ}} + b^S_{\mathrm{W}(\to\ell\nu)} + b^S_{\mathrm{other}})$.

The integral in Eq. (15) is approximated using MC integration by sampling the priors $\pi(\mathcal{L})$, and $\pi(\vec{\theta}_1, \cdots, \vec{\theta}_M)$ and averaging the multibin likelihood with respect to the sampled points $\{(\mathcal{L}, \vec{\theta}_1, \cdots, \vec{\theta}_M)\}$. The priors for the expected integrated luminosity $\mathcal{L}$, signal efficiencies ϵ, and simulated background counts $b^{\mathrm{region}}_{\mathrm{process,MC}}$ are modeled with gamma function densities,

$$\mathrm{Ga}(x, \gamma, \beta) = \beta^{-1}(x/\beta)^{\gamma-1} \exp(-x/\beta)/\Gamma(\gamma), \tag{16}$$

in which the mode is set to c and the variance to δc^2, where $c \pm \delta c$ denotes either the measured integrated luminosity, or for a given bin of a given region and process, the simulated signal efficiency, or the simulated background count. From $c \pm \delta c$, we calculate the gamma density parameters,

$$\gamma = [(k+2) + \sqrt{(k+2)^2 - 4}]/2, \tag{17}$$

$$\beta = [\sqrt{c^2 + 4\delta c^2} - c]/2, \tag{18}$$

where $k = (c/\delta c)^2$. For empty bins, we set $\gamma = 1$ and the bin value is constrained to zero by setting the β parameter to 10^{-4}.

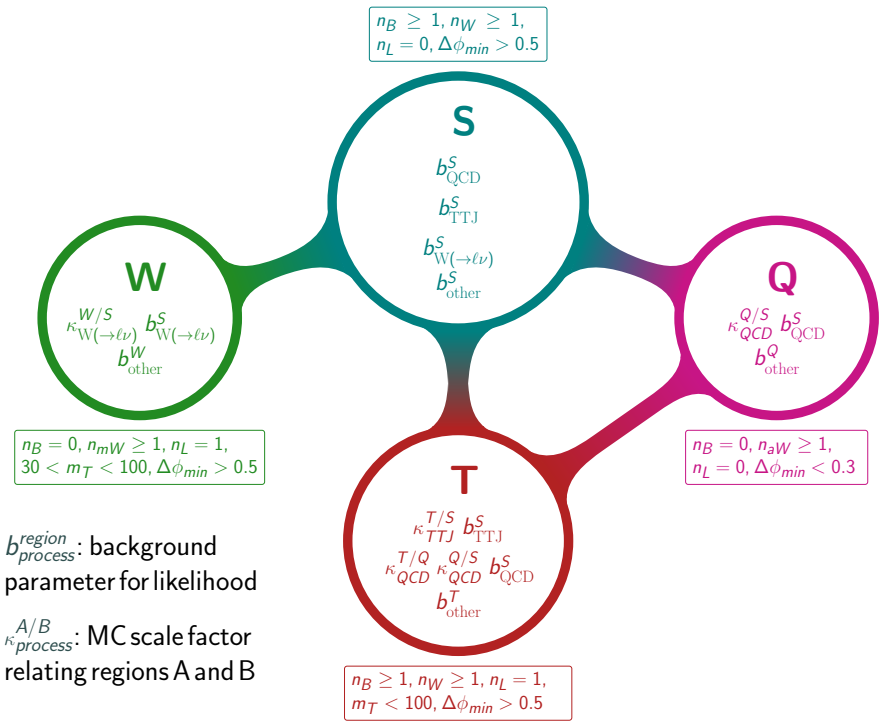

Figure 9: Graphical representation of the analysis method. The circles represent the signal (S) and control (Q, T, W) regions, with their definition summarized in the associated boxes. Listed inside each circle are the likelihood parameters relevant to that region: the bin-by-bin background parameters $b^{\mathrm{region}}_{\mathrm{process}}$ for the given region and background process, as well as the global scale factors $\kappa^{A/B}_{\mathrm{process}} = \sum_i b^A_{\mathrm{process,MC},i} / \sum_i b^B_{\mathrm{process,MC},i}$, where the sum is over all bins of the simulated data. A connection between two regions indicates that one or more parameters are shared. The total expected background, per (M_{R}, R^2) bin, is the sum of the terms shown for each region. Furthermore, associated with each bin of each region is an observed count, N^{region}, a simulated count, $N^{\mathrm{region}}_{\mathrm{process,MC}}$, and a count $N^{\mathrm{region}}_{\mathrm{other,MC}}$ equal to the sum of the smaller backgrounds, $\mathrm{Z}/\gamma^* \to \ell\bar{\ell}$+jets, diboson, triboson, and $\mathrm{t\bar{t}}V$, with associated parameter in the likelihood $b^{\mathrm{region}}_{\mathrm{other}}$.

For the signal efficiencies and backgrounds, the prior is modeled hierarchically,

$$\pi(\vec{\theta}_1, \cdots, \vec{\theta}_M) = \int \mathrm{d}\vec{c}_1 \cdots \int \mathrm{d}\vec{c}_M \int \mathrm{d}\vec{\phi} \left[\prod_{i=1}^{M} \pi(\vec{\theta}_i | \vec{c}_i) \right] \pi(\vec{c}_1, \cdots, \vec{c}_M | \vec{\phi}) \pi(\vec{\phi}), \tag{19}$$

where $\vec{\phi}$ represents parameters that characterize the independent sources of systematic uncertainty, described in Section 9. The integral in Eq. (19) is evaluated as follows: $\vec{\phi}$ values are sampled from $\pi(\vec{\phi})$ following the procedure described in Section 9, then $\vec{c}_i$ values from $\pi(\vec{c}_1, \cdots, \vec{c}_M | \vec{\phi})$, then $\vec{\theta}_i$ values from $\pi(\vec{\theta}_i | \vec{c}_i)$. The sampling from $\pi(\vec{\phi})$ and $\pi(\vec{\theta}_i | \vec{c}_i)$ is straightforward because the functional forms are known. However, the sampling of $\vec{c}_i$ requires running the analysis multiple times, yielding an ensemble of histograms in the (M_R, R^2) plane, which is the output of the procedure described in Section 9. Thereafter, the sampling, which yields the points $\{(\mathcal{L}, \vec{\theta}, \cdots, \vec{\theta}_M)\}$, proceeds as follows:

1. sample the integrated luminosity parameter;
2. sample the efficiency parameters, ϵ, for every bin and every signal model;
3. sample the background parameters $b^{\mathrm{region}}_{\mathrm{process,MC}}$ for every bin and every background;
4. scale $b^{Q}_{\mathrm{QCD,MC}}$ by a random number sampled from a gamma density of unit mode and standard deviation 0.36 in order to induce the 42% uncertainty in the multijet global scale factor $\kappa^{Q/S}_{\mathrm{QCD}}$ that accounts for deficiencies in the modeling of multijet production, as derived from the second cross-check mentioned in Section 6;
5. compute the κ parameters from the appropriate background sums, for example, $\kappa^{Q/S}_{\mathrm{QCD}} = \sum_i b^{Q}_{\mathrm{QCD,MC},i} / \sum b^{S}_{\mathrm{QCD,MC},i}$;
6. scale each κ value by a random number sampled from a gamma density with unit mode and standard deviation of either 0.5 or 1.0 for the bins in set 2 or set 3, respectively, to account for the larger uncertainties in the tails of the simulated distributions, and
7. sample the background parameters b^{S}_{QCD}, b^{S}_{TTJ}, and $b^{S}_{\mathrm{W}(\to \ell\nu)}$, from the Poisson models of the control regions; for example, for region Q, $\mathrm{Poisson}(N^{Q}, \kappa^{Q/S} b^{S}_{\mathrm{QCD}} + b^{Q}_{\mathrm{other}})$ is mapped to a posterior density in b^{S}_{QCD} using a flat prior in b^{S}_{QCD}, and b^{S}_{QCD} is sampled from the posterior density.

If no statistically significant signal is observed, we determine limits on the total signal cross section using the CLs criterion [80–82] and the test statistic $t_\sigma = 2\ln[L(\hat{\sigma})/L(\sigma)]$ when $0 \leq \hat{\sigma} \leq \sigma$, and $t_\sigma = 0$ when $\hat{\sigma} > \sigma$. Large values of t_σ indicate incompatibility between the best fit hypothesis $\sigma' = \hat{\sigma}$ and the hypothesis $\sigma' = \sigma$ being tested. Given the p-values $p_0 = \Pr(t_\sigma > t_{\sigma,\mathrm{obs}} | \sigma' = 0)$ and $p_\sigma = \Pr(t_\sigma > t_{\sigma,\mathrm{obs}} | \sigma' = \sigma)$, obtained by simulation, a 95% CLs upper limit on the cross section is obtained by solving $\mathrm{CLs}(\sigma) = p_\sigma / p_0 = 0.05$. The quantity $t_{\sigma,\mathrm{obs}}$ denotes the observed values of the test statistic, one for each hypothesis $\sigma' = \sigma$.

9 Systematic uncertainties

The input to the statistical analysis is an ensemble of histograms in the (M_R, R^2) plane that incorporate systematic uncertainties in the simulated signal and background samples. The independent systematic effects, described below, are sampled simultaneously. For each sampled

systematic effect, a Gaussian variate with zero mean and unit variance is used in the calculation of the random shift due to the systematic effect for all the signal and background models. Likewise, the same randomly sampled PDFs are used for all signal and background models. In this way, the statistical dependencies among all bins of the signal and background models are correctly, and automatically, modeled. The sampling of the systematic effects is repeated several hundred times.

In all cases, except for those associated with PDFs, the systematic uncertainties are in the scale factors (SF) applied to the simulated samples to correct them for modeling deficiencies. We consider the systematic uncertainties in the following quantities:

- **Jet energy scale:** The uncertainties are dependent on jet p_T and η [72].
- **Parton distribution functions:** We use 100 randomly sampled sets of PDFs from NNPDF23_lo_as_0130_qed [83], MSTW2008lo68cl [84], and CT10 [53]. The samples for the latter two are generated using the program HESSIAN2REPLICAS, recently released with LHAPDF6 [85]. Given a sampled set i, for PDF set K and the PDF set O with which the events were simulated, events are reweighted using the scale factors, $\mathrm{SF}_{K,i} = w_{K,i}/w_O$, where the weights w are products of the event-by-event PDFs for the colliding partons.
- **Trigger efficiency:** We take the uncertainty in each bin, as a function of H_T and leading jet p_T, to be the maximum of the statistical uncertainty in the efficiency after the baseline selection and the difference between the efficiencies before and after the baseline selection.
- **b tagging scale factors:** The b tagging performance differs between data and simulation, and differs between FULLSIM and FASTSIM, which is used to model signal processes. The simulated events are therefore corrected by applying jet flavor-, p_T-, and η-dependent data/FULLSIM and FULLSIM/FASTSIM scale factors on the b tagging or mistagging efficiency. The uncertainties in these scale factors are also jet flavor, p_T, and η dependent, and are of the order of a few percent [74].
- **W tagging scale factors:** The W boson tag efficiency, and the mistag efficiency for W boson tagging, W boson mass-tagging, and W boson anti-tagging differ between data and simulation, as well as between FULLSIM and FASTSIM. Data/FULLSIM and FULLSIM/FASTSIM scale factors, whose uncertainties are functions of jet p_T, are applied to the simulated samples.
- **Lepton identification:** For electrons, we use p_T- and η-dependent scale factors for the identification efficiency. The uncertainties are also p_T and η dependent [77]. The scale factor for the muon identification efficiency equals one and the corresponding uncertainties are negligible [78].
- **Initial-state radiation:** Deficiencies in the modeling of ISR are corrected by reweighting [19] the signal samples using an event weight that depends on the p_T of the recoiling system. The associated systematic uncertainty is equal to the difference $1 - w_{\mathrm{ISR}}$, where w_{ISR} is the ISR event weight.
- **Top quark transverse momentum:** Differential top quark pair production cross section analyses have shown that the shape of the p_T spectrum of top quarks in data is softer than predicted [86]. To account for this, we reweight events based on the p_T of the generator level t and $\bar{\mathrm{t}}$ quarks in the $\mathrm{t}\bar{\mathrm{t}}$ simulation. The uncertainty associated with this reweighting is taken to be equal to the full amount of the reweighting.
- **Pileup:** Simulated events are reweighted so that their vertex multiplicity distribu-

tion matches that observed in data. The minimum-bias cross section is varied by $\pm 5\%$, thereby changing the shape of the vertex multiplicity distribution and therefore the weights.

- **Multijet spectrum:** The cross-checks described in Section 6 showed that there is a 42% uncertainty in the multijet scale factor κ between the S and Q regions. This uncertainty is incorporated by increasing the uncertainty in the κ parameter, as described in Section 8.
- **Z($\to \nu\overline{\nu}$)+jets prediction:** About 8% of the background in the signal region is composed of Z($\to \nu\overline{\nu}$)+jets events. Since we require the presence of at least one b-tagged jet, and given the known deficiency in modeling Z production in association with heavy flavor quarks, we include an extra systematic uncertainty in the Z($\to \nu\overline{\nu}$)+jets contribution. This uncertainty is estimated using a data control region enriched in Z($\to \ell\overline{\ell}$)+jets, required to have exactly two tight leptons with same flavor (e or μ) and opposite charge, $60 < m_{\ell\overline{\ell}} < 120\,\text{GeV}$, at least one b-tagged jet, and at least one W mass-tagged jet. We estimate the uncertainty by first computing bin-by-bin data/simulation ratios in this control region. Then, we take the uncertainty in the ratio in each bin as the standard deviation of a Gaussian density, normalized to the number of events in that bin. Finally, the Gaussian densities from all bins are superposed, and the uncertainty is taken to be the magnitude of the 68% band around a ratio of unity.

As noted above, all systematic effects are varied simultaneously across (M_{R}, R^2) bins. However, to assess the effect of each systematic uncertainty individually, each one is varied by one standard deviation up and down. The effect on the background count and signal efficiency in the signal region is shown in Table 4. The signal values are obtained from averaging over all mass points in the T1ttcc model ($\Delta m = 25\,\text{GeV}$) plane. The PDF systematic uncertainties are obtained by running over 100 different members from the three PDF sets and fitting a Gaussian function to the efficiency distribution. The last line in the table corresponds to the full sampling of the systematic uncertainties. To obtain this value, we again fit a Gaussian function to the efficiency distribution obtained from the full systematic sampling including 500 variations. Although the effects of some of these systematic uncertainties on the backgrounds are large, they do not influence our results greatly because only the ratios of simulated background counts enter the statistical analysis, not the absolute values. Therefore, most of the systematic effects cancel. The statistical precision on the number of events in the control regions is the leading uncertainty in the background prediction for the search bins at large M_{R} or R^2. The dominant systematic uncertainty in the signal efficiency arises from the PDFs.

10 Results and interpretation

Our background predictions for each bin in the (M_{R}, R^2) plane are presented in Fig. 10 and in Table 5, which also lists the observed event yield in each bin. The background predictions are presented as the mean and standard deviation as determined from the background prior $\pi(\theta)$ described in Section 8. The observed event yields are found to be in agreement with the predicted backgrounds from SM processes. Consequently, no evidence of a signal is observed.

We interpret our results in terms of the simplified model spectra T1ttcc and T1t1t, whose diagrams are shown in Fig. 1. These models each have three mass parameters: the gluino, top squark, and LSP masses. The mass of the gluino is varied between 600 and 1300 GeV and that of the LSP between 1 and 500 GeV, while the mass difference between the top squark and the LSP, Δm, is fixed at 10, 25, or 80 GeV for the T1ttcc model, and at 175 GeV for the T1t1t model.

Table 4: Summary of ± 1 standard deviation systematic uncertainties for the average signal efficiency over all mass assumptions in the T1ttcc model ($\Delta m = 25\,\text{GeV}$), and for the total background count in the signal region, unless indicated otherwise, as determined from simulation.

Systematic effect	Signal (%)	Background (%)
Jet energy scale	$+2.2\ -2.1$	$+10.9\ -5.2$
Trigger	$+1.1\ -3.3$	$+3.4\ -5.7$
b tagging FULLSIM	$+2.1\ -2.3$	$+3.9\ -4.0$
b tagging FASTSIM	$+1.2\ -1.3$	—
W tag efficiency FULLSIM	$+9.0\ -8.9$	$+4.6\ -4.6$
W tag efficiency FASTSIM	$+2.2\ -2.2$	—
W tag mistag efficiency FULLSIM	—	$+1.4\ -1.4$
W anti-tag mistag efficiency FULLSIM (Q region only)	—	$+2.6\ -2.6$
W mass-tag mistag efficiency FULLSIM (W region only)	—	$+2.3\ -2.3$
Electron identification (T and W region only)	—	$+0.2\ -0.2$
Pileup	$+0.5\ -0.5$	$+1.0\ -1.1$
ISR	$+6.6\ -6.6$	—
Top quark p_{T}	—	$+20.5\ -14.4$
$\mathrm{Z}(\to \nu\bar{\nu})+$ heavy flavor	—	$+4.0\ -4.0$
PDF	20.7	10.7
All	24.4	22.1

Table 5: Event yields for the predicted backgrounds and for the data in each of the signal bins in R^2 and M_{R}. The uncertainties in the predictions are the combined statistical and systematic uncertainties obtained using the sampling procedure described in the text.

R^2	M_{R} (GeV)	$\mathrm{t\bar{t}}$	Multijet	$\mathrm{W}(\to \ell\nu)$	Other	Total	Observed
[0.08, 0.12[	[800, 1000[	47.1 ± 8.6	21.1 ± 32.0	6.1 ± 1.9	6.0 ± 2.3	80.2 ± 33.4	75
	[1000, 1200[	15.2 ± 4.1	4.7 ± 9.9	1.9 ± 0.9	2.2 ± 0.9	24.0 ± 10.6	24
	[1200, 1600[	7.3 ± 4.8	1.4 ± 0.9	1.3 ± 1.0	1.4 ± 0.7	11.4 ± 5.1	10
	[1600, 2000[	0.8 ± 1.2	0.2 ± 0.2	0.4 ± 0.5	0.1 ± 0.0	1.5 ± 1.3	0
	[2000, 4000]	0.8 ± 1.1	0.0 ± 0.1	0.4 ± 0.6	0.1 ± 0.1	1.4 ± 1.3	0
[0.12, 0.16[	[800, 1000[	15.5 ± 4.2	2.5 ± 1.2	1.1 ± 0.8	2.8 ± 1.2	21.9 ± 4.8	34
	[1000, 1200[	3.4 ± 1.8	0.5 ± 0.3	1.3 ± 0.6	1.2 ± 0.7	6.4 ± 2.0	8
	[1200, 1600[	2.8 ± 2.3	0.2 ± 0.1	0.6 ± 0.5	0.6 ± 0.4	4.1 ± 2.3	3
	[1600, 2000[	0.8 ± 1.2	0.0 ± 0.1	0.2 ± 0.3	0.1 ± 0.0	1.1 ± 1.2	0
	[2000, 4000]	0.8 ± 1.1	0.0 ± 0.0	0.2 ± 0.4	0.0 ± 0.0	1.0 ± 1.1	0
[0.16, 0.24[	[800, 1000[	9.1 ± 5.8	0.7 ± 0.4	1.8 ± 1.4	2.4 ± 1.1	14.0 ± 6.0	16
	[1000, 1200[	2.5 ± 2.4	0.2 ± 0.1	0.5 ± 0.5	1.5 ± 0.8	4.7 ± 2.5	4
	[1200, 1600[	0.9 ± 1.0	0.1 ± 0.1	1.3 ± 0.9	0.2 ± 0.2	2.5 ± 1.4	2
	[1600, 2000[	0.9 ± 1.6	0.0 ± 0.0	0.2 ± 0.3	0.0 ± 0.0	1.1 ± 1.7	1
	[2000, 4000]	0.9 ± 1.3	0.0 ± 0.0	0.2 ± 0.3	0.0 ± 0.0	1.1 ± 1.3	0
[0.24, 0.5[	[800, 1000[	7.4 ± 7.0	0.1 ± 0.1	0.9 ± 1.2	2.1 ± 1.0	10.4 ± 7.2	8
	[1000, 1200[	1.3 ± 1.4	0.0 ± 0.0	0.9 ± 1.0	0.6 ± 0.3	2.7 ± 1.6	0
	[1200, 1600[	0.8 ± 1.4	0.0 ± 0.0	0.4 ± 0.6	0.2 ± 0.2	1.5 ± 1.5	1
	[1600, 2000[	0.8 ± 1.1	0.0 ± 0.0	0.2 ± 0.2	0.1 ± 0.0	1.0 ± 1.1	0
	[2000, 4000]	0.8 ± 1.2	0.0 ± 0.0	0.2 ± 0.3	0.0 ± 0.0	1.1 ± 1.2	0
[0.5, 1]	[800, 1000[	2.0 ± 1.9	0.0 ± 0.0	0.4 ± 0.6	0.5 ± 0.3	2.9 ± 2.0	0
	[1000, 1200[	0.9 ± 1.3	0.0 ± 0.0	0.2 ± 0.4	0.1 ± 0.1	1.2 ± 1.4	1
	[1200, 1600[	0.9 ± 1.2	0.0 ± 0.0	0.2 ± 0.3	0.1 ± 0.1	1.2 ± 1.3	0
	[1600, 2000[	0.8 ± 1.1	0.0 ± 0.0	0.2 ± 0.5	0.0 ± 0.0	1.0 ± 1.2	0
	[2000, 4000]	0.8 ± 1.0	0.0 ± 0.0	0.2 ± 0.3	0.0 ± 0.0	1.0 ± 1.0	0

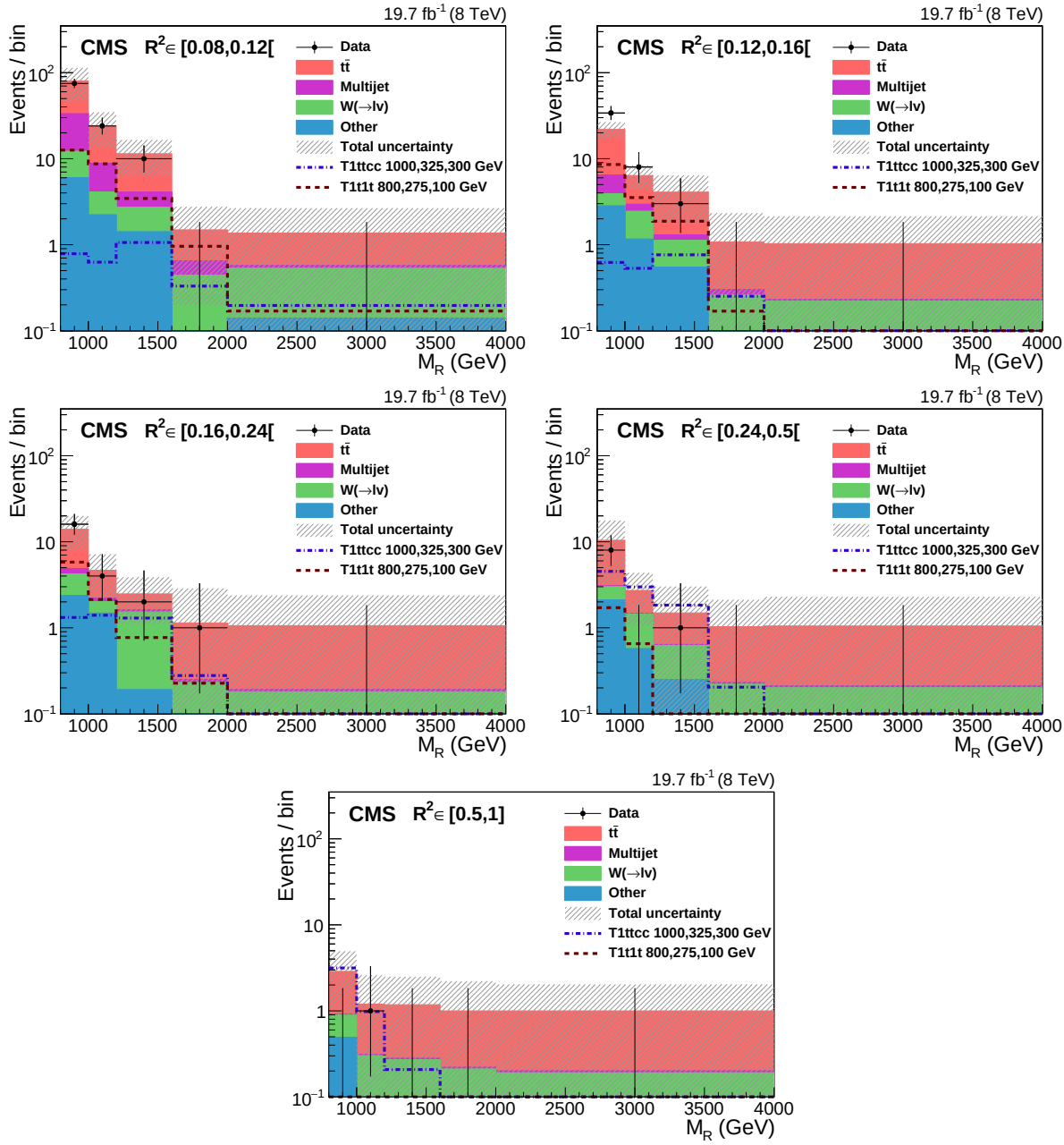

Figure 10: Background predictions and observations. The results are shown in bins of M_R for each R^2 bin. The hatched band represents the total uncertainty in the background prediction. Overlaid are two signal distributions corresponding to the T1ttcc model with $m_{\tilde{g}} = 1$ TeV, $m_{\tilde{t}} = 325$ GeV and $m_{\tilde{\chi}_1^0} = 300$ GeV, and the T1t1t model with $m_{\tilde{g}} = 800$ GeV, $m_{\tilde{t}} = 275$ GeV and $m_{\tilde{\chi}_1^0} = 100$ GeV.

In both models the gluino is assumed to decay 100% of the time into a top squark and a top quark.

To illustrate the expected signal sensitivity, we show in Fig. 11 the signal efficiencies as a function of the gluino and neutralino masses, for the T1ttcc model, to which this analysis is particularly sensitive, and for the T1t1t model. Efficiencies of up to 6% in the most boosted regimes are reached. For the T1ttcc model a drop in efficiency is observed for the region of model parameter space with the lowest neutralino mass ($m_{\tilde{\chi}_1^0} = 1\,\text{GeV}$), which can be explained by Lorentz boosts. For LSP masses higher than the mass of the charm quark, the LSP will assume most of the momentum. For the bins with the lowest LSP mass, however, the LSP and the charm quark have about equal mass, so that after the boost they will share the momentum about equally. This results in a softer $E_{\text{T}}^{\text{miss}}$ spectrum and therefore a lower R^2 value, which reduces the efficiency substantially.

Figure 12 shows the observed 95% confidence level (CL) upper limit on the signal cross section as a function of the gluino and neutralino masses, obtained using the CLs method described briefly in Section 8, for the T1t1t model and for the T1ttcc model with $\Delta m = 10$, 25, and 80 GeV. Additionally, the figure also shows contours corresponding to the observed and expected lower limits, including their uncertainties, on the gluino and neutralino masses. This analysis has made significant inroads into the parameter space of the T1ttcc model. Gluinos with mass up to about 1.1 TeV have been excluded for neutralinos with mass less than about 400 GeV when the top squark decays to a charm quark and a neutralino and $\Delta m < 80\,\text{GeV}$. This also means that top squarks with masses up to about 400 GeV have been excluded for small mass differences with the LSP, given the existence of a gluino with mass less than about 1.1 TeV. Similarly, for the T1t1t model, top squarks with a mass up to about 300 GeV have been excluded for the scenarios with $\Delta m = 175\,\text{GeV}$ and gluino mass less than 700 GeV. The observed limit for this model is lower than the expected limit because of the small excess in the low M_{R} bins for $0.12 \leq R^2 < 0.16$, which are among the most sensitive bins for the T1t1t model.

11 Summary

We have presented a search for new physics in hadronic final states with at least one boosted W boson and a b-tagged jet using data binned at high values of the razor kinematic variables, M_{R} and R^2. The analysis uses 19.7 fb^{-1} of 8 TeV proton-proton collision data collected by the CMS experiment. The SM backgrounds are estimated using control regions in data. Scale factors, derived from simulations, connect these control regions to the signal region. The observations are found to be consistent with the SM expectation, as shown in Fig. 10 and Table 5. The results, which are encapsulated in a binned likelihood, are interpreted in terms of supersymmetric models describing pair production of heavy gluinos decaying to boosted top quarks. Limits are set on the gluino and neutralino masses using the CLs criterion on the gluino-neutralino mass plane, as shown in Fig. 12. Assuming that the gluino always decays into a top squark and a top quark, this analysis excludes gluino masses up to 1.1 TeV for top squarks with mass up to about 450 GeV that decay exclusively to a charm quark and a neutralino. In this scenario, the mass difference considered between the top squark and neutralino is less than 80 GeV. This analysis also excludes gluino masses up to 700 GeV when the top squark decays solely to a top quark and a neutralino, and the mass difference between the top squark and the neutralino is around the top quark mass.

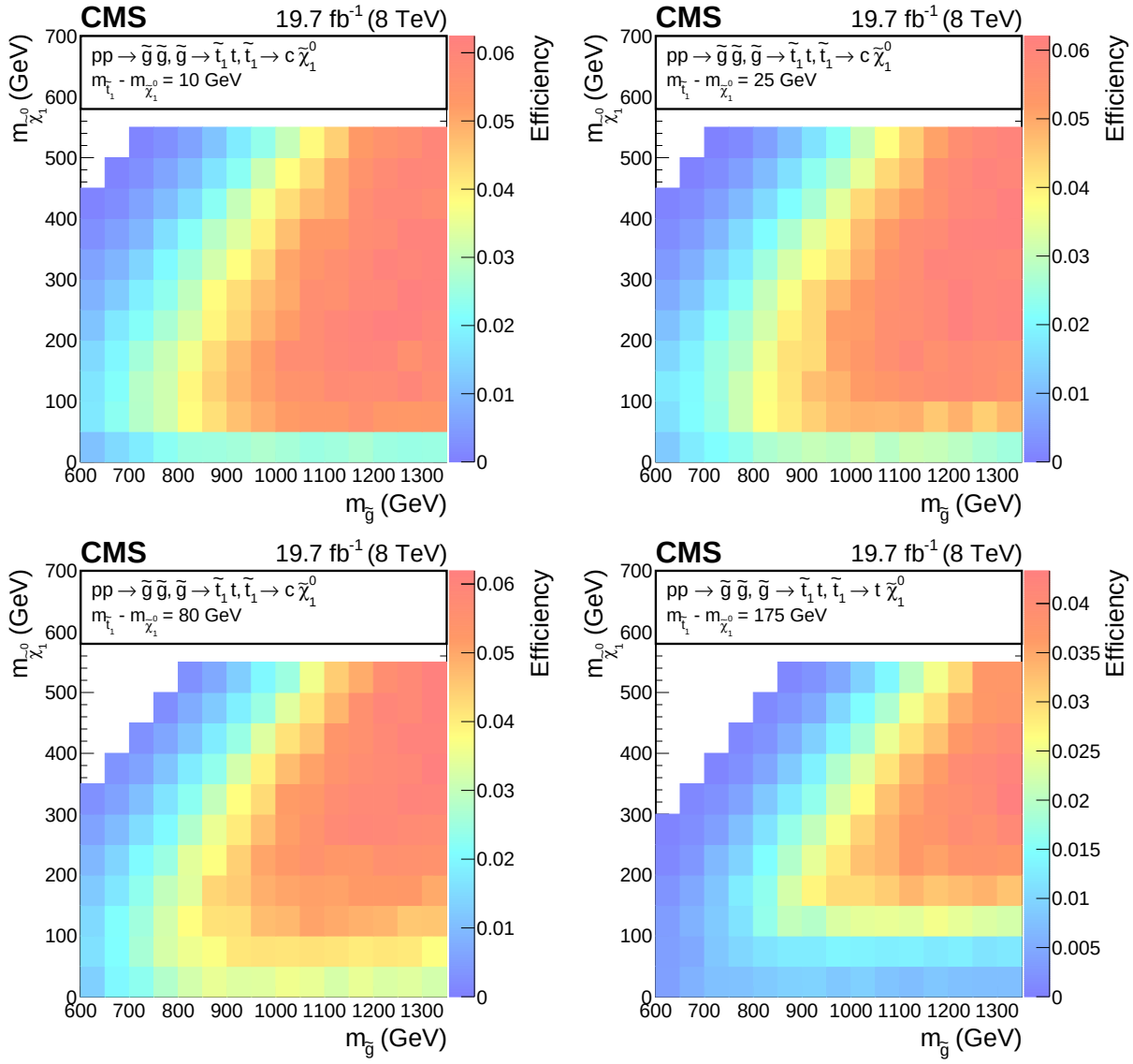

Figure 11: Signal efficiency for the T1ttcc and T1t1t simplified model spectra, as a function of the gluino and neutralino masses. Three mass splittings between top squark and LSP are considered for the T1ttcc model: 10, 25, and 80 GeV, shown on the top left, top right, and bottom left, respectively. The efficiency for the T1t1t model with a mass splitting of 175 GeV is shown on the bottom right.

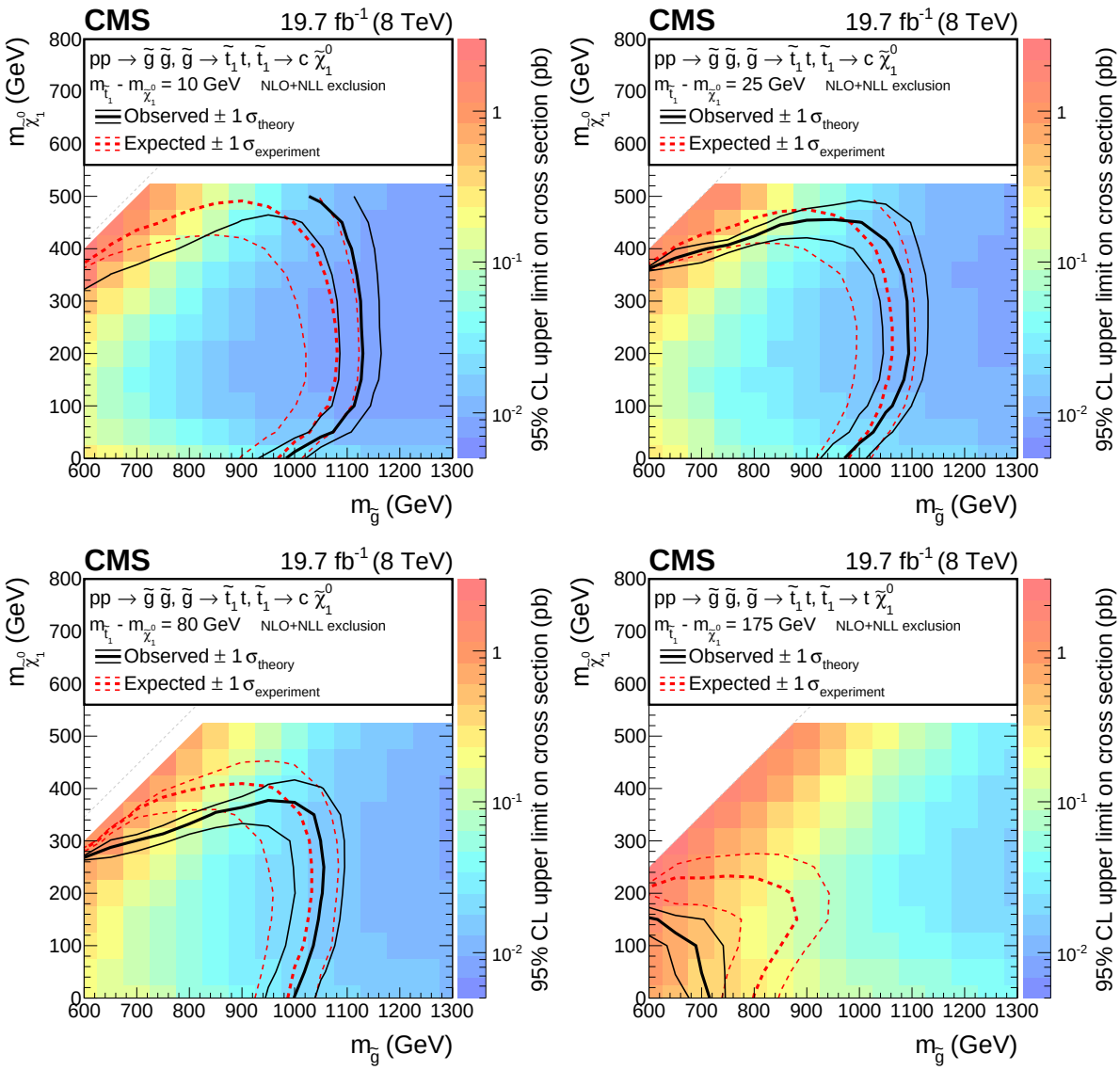

Figure 12: Observed upper limit (CLs method, 95% CL) on the signal cross section as a function of the gluino and neutralino masses for the T1ttcc model with $\Delta m = 10, 25,$ and $80\,\mathrm{GeV}$ (top left, top right, bottom left) and for the T1t1t model with $\Delta m = 175\,\mathrm{GeV}$ (bottom right). Also shown are the contours corresponding to the observed and expected lower limits, including their uncertainties, on the gluino and neutralino masses.

Acknowledgements

We congratulate our colleagues in the CERN accelerator departments for the excellent performance of the LHC and thank the technical and administrative staffs at CERN and at other CMS institutes for their contributions to the success of the CMS effort. In addition, we gratefully acknowledge the computing centres and personnel of the Worldwide LHC Computing Grid for delivering so effectively the computing infrastructure essential to our analyses. Finally, we acknowledge the enduring support for the construction and operation of the LHC and the CMS detector provided by the following funding agencies: the Austrian Federal Ministry of Science, Research and Economy and the Austrian Science Fund; the Belgian Fonds de la Recherche Scientifique, and Fonds voor Wetenschappelijk Onderzoek; the Brazilian Funding Agencies (CNPq, CAPES, FAPERJ, and FAPESP); the Bulgarian Ministry of Education and Science; CERN; the Chinese Academy of Sciences, Ministry of Science and Technology, and National Natural Science Foundation of China; the Colombian Funding Agency (COLCIENCIAS); the Croatian Ministry of Science, Education and Sport, and the Croatian Science Foundation; the Research Promotion Foundation, Cyprus; the Ministry of Education and Research, Estonian Research Council via IUT23-4 and IUT23-6 and European Regional Development Fund, Estonia; the Academy of Finland, Finnish Ministry of Education and Culture, and Helsinki Institute of Physics; the Institut National de Physique Nucléaire et de Physique des Particules / CNRS, and Commissariat à l'Énergie Atomique et aux Énergies Alternatives / CEA, France; the Bundesministerium für Bildung und Forschung, Deutsche Forschungsgemeinschaft, and Helmholtz-Gemeinschaft Deutscher Forschungszentren, Germany; the General Secretariat for Research and Technology, Greece; the National Scientific Research Foundation, and National Innovation Office, Hungary; the Department of Atomic Energy and the Department of Science and Technology, India; the Institute for Studies in Theoretical Physics and Mathematics, Iran; the Science Foundation, Ireland; the Istituto Nazionale di Fisica Nucleare, Italy; the Ministry of Science, ICT and Future Planning, and National Research Foundation (NRF), Republic of Korea; the Lithuanian Academy of Sciences; the Ministry of Education, and University of Malaya (Malaysia); the Mexican Funding Agencies (CINVESTAV, CONACYT, SEP, and UASLP-FAI); the Ministry of Business, Innovation and Employment, New Zealand; the Pakistan Atomic Energy Commission; the Ministry of Science and Higher Education and the National Science Centre, Poland; the Fundação para a Ciência e a Tecnologia, Portugal; JINR, Dubna; the Ministry of Education and Science of the Russian Federation, the Federal Agency of Atomic Energy of the Russian Federation, Russian Academy of Sciences, and the Russian Foundation for Basic Research; the Ministry of Education, Science and Technological Development of Serbia; the Secretaría de Estado de Investigación, Desarrollo e Innovación and Programa Consolider-Ingenio 2010, Spain; the Swiss Funding Agencies (ETH Board, ETH Zurich, PSI, SNF, UniZH, Canton Zurich, and SER); the Ministry of Science and Technology, Taipei; the Thailand Center of Excellence in Physics, the Institute for the Promotion of Teaching Science and Technology of Thailand, Special Task Force for Activating Research and the National Science and Technology Development Agency of Thailand; the Scientific and Technical Research Council of Turkey, and Turkish Atomic Energy Authority; the National Academy of Sciences of Ukraine, and State Fund for Fundamental Researches, Ukraine; the Science and Technology Facilities Council, UK; the US Department of Energy, and the US National Science Foundation.

Individuals have received support from the Marie-Curie programme and the European Research Council and EPLANET (European Union); the Leventis Foundation; the A. P. Sloan Foundation; the Alexander von Humboldt Foundation; the Belgian Federal Science Policy Office; the Fonds pour la Formation à la Recherche dans l'Industrie et dans l'Agriculture (FRIA-Belgium); the Agentschap voor Innovatie door Wetenschap en Technologie (IWT-Belgium); the

Ministry of Education, Youth and Sports (MEYS) of the Czech Republic; the Council of Science and Industrial Research, India; the HOMING PLUS programme of the Foundation for Polish Science, cofinanced from European Union, Regional Development Fund; the OPUS programme of the National Science Center (Poland); the Compagnia di San Paolo (Torino); MIUR project 20108T4XTM (Italy); the Thalis and Aristeia programmes cofinanced by EU-ESF and the Greek NSRF; the National Priorities Research Program by Qatar National Research Fund; the Rachadapisek Sompot Fund for Postdoctoral Fellowship, Chulalongkorn University (Thailand); the Chulalongkorn Academic into Its 2nd Century Project Advancement Project (Thailand); and the Welch Foundation, contract C-1845.

References

[1] J. Wess and B. Zumino, "Supergauge transformations in four-dimensions", *Nucl. Phys. B* **70** (1974) 39, doi:10.1016/0550-3213(74)90355-1.

[2] Y. A. Gol'fand and E. P. Likhtman, "Extension of the algebra of Poincaré group generators and violation of P invariance", *JETP Lett.* **13** (1971) 323.

[3] D. V. Volkov and V. P. Akulov, "Possible universal neutrino interaction", *JETP Lett.* **16** (1972) 438.

[4] A. H. Chamseddine, R. L. Arnowitt, and P. Nath, "Locally supersymmetric grand unification", *Phys. Rev. Lett.* **49** (1982) 970, doi:10.1103/PhysRevLett.49.970.

[5] G. L. Kane, C. F. Kolda, L. Roszkowski, and J. D. Wells, "Study of constrained minimal supersymmetry", *Phys. Rev. D* **49** (1994) 6173, doi:10.1103/PhysRevD.49.6173, arXiv:hep-ph/9312272.

[6] P. Fayet, "Supergauge invariant extension of the Higgs mechanism and a model for the electron and its neutrino", *Nucl. Phys. B* **90** (1975) 104, doi:10.1016/0550-3213(75)90636-7.

[7] R. Barbieri, S. Ferrara, and C. A. Savoy, "Gauge models with spontaneously broken local supersymmetry", *Phys. Lett. B* **119** (1982) 343, doi:10.1016/0370-2693(82)90685-2.

[8] L. J. Hall, J. D. Lykken, and S. Weinberg, "Supergravity as the messenger of supersymmetry breaking", *Phys. Rev. D* **27** (1983) 2359, doi:10.1103/PhysRevD.27.2359.

[9] P. Ramond, "Dual theory for free fermions", *Phys. Rev. D* **3** (1971) 2415, doi:10.1103/PhysRevD.3.2415.

[10] R. Barbieri and D. Pappadopulo, "S-particles at their naturalness limits", *JHEP* **10** (2009) 061, doi:10.1088/1126-6708/2009/10/061, arXiv:0906.4546.

[11] M. Papucci, J. T. Ruderman, and A. Weiler, "Natural SUSY endures", *JHEP* **09** (2012) 035, doi:10.1007/JHEP09(2012)035, arXiv:1110.6926.

[12] ATLAS Collaboration, "Search for direct third-generation squark pair production in final states with missing transverse momentum and two b-jets in $\sqrt{s} = 8$ TeV pp collisions with the ATLAS detector", *JHEP* **10** (2013) 189, doi:10.1007/JHEP10(2013)189, arXiv:1308.2631.

[13] ATLAS Collaboration, "Search for direct top-squark pair production in final states with two leptons in pp collisions at $\sqrt{s} = 8$ TeV with the ATLAS detector", *JHEP* **06** (2014) 124, doi:10.1007/JHEP06(2014)124, arXiv:1403.4853.

[14] ATLAS Collaboration, "Search for direct pair production of the top squark in all-hadronic final states in proton-proton collisions at $\sqrt{s} = 8$ TeV with the ATLAS detector", *JHEP* **09** (2014) 015, doi:10.1007/JHEP09(2014)015, arXiv:1406.1122.

[15] ATLAS Collaboration, "Measurement of the $t\bar{t}$ production cross-section using $e\mu$ events with b-tagged jets in pp collisions at $\sqrt{s} = 7$ and 8 TeV with the ATLAS detector", *Eur. Phys. J. C* **74** (2014) 3109, doi:10.1140/epjc/s10052-014-3109-7, arXiv:1406.5375.

[16] ATLAS Collaboration, "Search for top squark pair production in final states with one isolated lepton, jets, and missing transverse momentum in $\sqrt{s} = 8\,\text{TeV}$ pp collisions with the ATLAS detector", *JHEP* **11** (2014) 118, doi:10.1007/JHEP11(2014)118, arXiv:1407.0583.

[17] ATLAS Collaboration, "Search for direct top squark pair production in events with a Z boson, b-jets and missing transverse momentum in $\sqrt{s} = 8\,\text{TeV}$ pp collisions with the ATLAS detector", *Eur. Phys. J. C* **74** (2014) 2883, doi:10.1140/epjc/s10052-014-2883-6, arXiv:1403.5222.

[18] ATLAS Collaboration, "Search for strong production of supersymmetric particles in final states with missing transverse momentum and at least three b-jets at $\sqrt{s} = 8\,\text{TeV}$ proton-proton collisions with the ATLAS detector", *JHEP* **10** (2014) 024, doi:10.1007/JHEP10(2014)024, arXiv:1407.0600.

[19] CMS Collaboration, "Search for top-squark pair production in the single-lepton final state in pp collisions at $\sqrt{s} = 8\,\text{TeV}$", *Eur. Phys. J. C* **73** (2013) 2677, doi:10.1140/epjc/s10052-013-2677-2, arXiv:1308.1586.

[20] CMS Collaboration, "Search for top squark and higgsino production using diphoton Higgs boson decays", *Phys. Rev. Lett.* **112** (2014) 161802, doi:10.1103/PhysRevLett.112.161802, arXiv:1312.3310.

[21] CMS Collaboration, "Search for top-squark pairs decaying into Higgs or Z bosons in pp collisions at $\sqrt{s} = 8\,\text{TeV}$", *Phys. Lett. B* **736** (2014) 371, doi:10.1016/j.physletb.2014.07.053, arXiv:1405.3886.

[22] CMS Collaboration, "Searches for supersymmetry using the M_{T2} variable in hadronic events produced in pp collisions at 8 TeV", *JHEP* **05** (2015) 078, doi:10.1007/JHEP05(2015)078, arXiv:1502.04358.

[23] CMS Collaboration, "Search for supersymmetry in events with soft leptons, low jet multiplicity, and missing transverse momentum in proton-proton collisions at $\sqrt{s} = 8\,\text{TeV}$", (2015). arXiv:1512.08002. Submitted to Phys. Lett. B.

[24] S. P. Martin, "Compressed supersymmetry and natural neutralino dark matter from top squark-mediated annihilation to top quarks", *Phys. Rev. D* **75** (2007) 115005, doi:10.1103/PhysRevD.75.115005, arXiv:hep-ph/0703097.

[25] S. P. Martin, "The top squark-mediated annihilation scenario and direct detection of dark matter in compressed supersymmetry", *Phys. Rev. D* **76** (2007) 095005, doi:10.1103/PhysRevD.76.095005, arXiv:0707.2812.

[26] M. Carena, A. Freitas, and C. E. M. Wagner, "Light stop searches at the LHC in events with one hard photon or jet and missing energy", *JHEP* **10** (2008) 109, doi:10.1088/1126-6708/2008/10/109, arXiv:0808.2298.

[27] CMS Collaboration, "Searches for third-generation squark production in fully hadronic final states in proton-proton collisions at $\sqrt{s} = 8\,\text{TeV}$", *JHEP* **06** (2015) 116, doi:10.1007/JHEP06(2015)116, arXiv:1503.08037.

[28] ATLAS Collaboration, "Search for pair-produced third-generation squarks decaying via charm quarks or in compressed supersymmetric scenarios in pp collisions at $\sqrt{s} = 8\,\text{TeV}$ with the ATLAS detector", *Phys. Rev. D* **90** (2014) 052008, doi:10.1103/PhysRevD.90.052008, arXiv:1407.0608.

[29] LHC New Physics Working Group Collaboration, "Simplified models for LHC new physics searches", *J. Phys. G* **39** (2012) 105005, doi:10.1088/0954-3899/39/10/105005, arXiv:1105.2838.

[30] D. Alves, E. Izaguirre, and J. G. Wacker, "Where the sidewalk ends: jets and missing energy search strategies for the 7 TeV LHC", *JHEP* **10** (2011) 012, doi:10.1007/JHEP10(2011)012, arXiv:1102.5338.

[31] J. Alwall, P. Schuster, and N. Toro, "Simplified models for a first characterization of new physics at the LHC", *Phys. Rev. D* **79** (2009) 075020, doi:10.1103/PhysRevD.79.075020, arXiv:0810.3921.

[32] J. Alwall, M.-P. Le, M. Lisanti, and J. G. Wacker, "Model-independent jets plus missing energy searches", *Phys. Rev. D* **79** (2009) 015005, doi:10.1103/PhysRevD.79.015005, arXiv:0809.3264.

[33] N. Arkani-Hamed et al., "MARMOSET: The path from LHC data to the new Standard Model via on-shell effective theories", (2007). arXiv:hep-ph/0703088.

[34] CMS Collaboration, "Interpretation of searches for supersymmetry with simplified models", *Phys. Rev. D* **88** (2013) 052017, doi:10.1103/PhysRevD.88.052017, arXiv:1301.2175.

[35] S. D. Ellis, C. K. Vermilion, and J. R. Walsh, "Techniques for improved heavy particle searches with jet substructure", *Phys. Rev. D* **80** (2009) 051501, doi:10.1103/PhysRevD.80.051501, arXiv:0903.5081.

[36] S. D. Ellis, C. K. Vermilion, and J. R. Walsh, "Recombination algorithms and jet substructure: Pruning as a tool for heavy particle searches", *Phys. Rev. D* **81** (2010) 094023, doi:10.1103/PhysRevD.81.094023, arXiv:0912.0033.

[37] CMS Collaboration, "Studies of jet mass in dijet and W/Z+jet events", *JHEP* **05** (2013) 090, doi:10.1007/JHEP05(2013)090, arXiv:1303.4811.

[38] J. Thaler and K. Van Tilburg, "Identifying boosted objects with N-subjettiness", *JHEP* **03** (2011) 015, doi:10.1007/JHEP03(2011)015, arXiv:1011.2268.

[39] C. Rogan, "Kinematical variables towards new dynamics at the LHC", (2010). arXiv:1006.2727.

[40] CMS Collaboration, "Inclusive search for supersymmetry using the razor variables in pp collisions at $\sqrt{s} = 7\,\text{TeV}$", *Phys. Rev. Lett.* **111** (2013) 081802, doi:10.1103/PhysRevLett.111.081802, arXiv:1212.6961.

[41] CMS Collaboration, "Inclusive search for squarks and gluinos in pp collisions at $\sqrt{s} = 7\,\text{TeV}$", *Phys. Rev. D* **85** (2012) 012004, doi:10.1103/PhysRevD.85.012004, arXiv:1107.1279.

[42] CMS Collaboration, "Search for supersymmetry with razor variables in pp collisions at $\sqrt{s} = 7\,\text{TeV}$", *Phys. Rev. D* **90** (2014) 112001, doi:10.1103/PhysRevD.90.112001, arXiv:1405.3961.

[43] CMS Collaboration, "Search for supersymmetry using razor variables in events with bb-tagged jets in pp collisions at $\sqrt{s} = 8\,\text{TeV}$", *Phys. Rev. D* **91** (2015) 052018, doi:10.1103/PhysRevD.91.052018, arXiv:1502.00300.

[44] CMS Collaboration, "The CMS experiment at the CERN LHC", *JINST* **3** (2008) S08004, doi:10.1088/1748-0221/3/08/S08004.

[45] CMS Collaboration, "Particle–flow event reconstruction in CMS and performance for jets, taus, and $E_{\mathrm{T}}^{\mathrm{miss}}$", CMS Physics Analysis Summary CMS-PAS-PFT-09-001, 2009.

[46] CMS Collaboration, "Commissioning of the particle–flow event reconstruction with the first LHC collisions recorded in the CMS detector", CMS Physics Analysis Summary CMS-PAS-PFT-10-001, 2010.

[47] J. Alwall et al., "MadGraph 5: Going beyond", *JHEP* **06** (2011) 128, doi:10.1007/JHEP06(2011)128, arXiv:1106.0522.

[48] J. Alwall et al., "The automated computation of tree-level and next-to-leading order differential cross sections, and their matching to parton shower simulations", *JHEP* **07** (2014) 079, doi:10.1007/JHEP07(2014)079, arXiv:1405.0301.

[49] J. Pumplin et al., "New generation of parton distributions with uncertainties from global QCD analysis", *JHEP* **07** (2002) 012, doi:10.1088/1126-6708/2002/07/012, arXiv:hep-ph/0201195.

[50] T. Sjöstrand, S. Mrenna, and P. Z. Skands, "PYTHIA 6.4 physics and manual", *JHEP* **05** (2006) 026, doi:10.1088/1126-6708/2006/05/026, arXiv:hep-ph/0603175.

[51] S. Alioli, P. Nason, C. Oleari, and E. Re, "NLO single-top production matched with shower in POWHEG: *s*- and *t*-channel contributions", *JHEP* **09** (2009) 111, doi:10.1088/1126-6708/2009/09/111, arXiv:0907.4076. [Erratum: doi:10.1007/JHEP02(2010)011].

[52] E. Re, "Single-top Wt-channel production matched with parton showers using the POWHEG method", *Eur. Phys. J. C* **71** (2011) 1547, doi:10.1140/epjc/s10052-011-1547-z, arXiv:1009.2450.

[53] H.-L. Lai et al., "New parton distributions for collider physics", *Phys. Rev. D* **82** (2010) 074024, doi:10.1103/PhysRevD.82.074024, arXiv:1007.2241.

[54] M. Kramer et al., "Supersymmetry production cross sections in pp collisions at $\sqrt{s} = 7\,\mathrm{TeV}$", (2012). arXiv:1206.2892.

[55] W. Beenakker, R. Hopker, M. Spira, and P. M. Zerwas, "Squark and gluino production at hadron colliders", *Nucl. Phys. B* **492** (1997) 51, doi:10.1016/S0550-3213(97)80027-2, arXiv:hep-ph/9610490.

[56] A. Kulesza and L. Motyka, "Threshold resummation for squark-antisquark and gluino-pair production at the LHC", *Phys. Rev. Lett.* **102** (2009) 111802, doi:10.1103/PhysRevLett.102.111802, arXiv:0807.2405.

[57] A. Kulesza and L. Motyka, "Soft gluon resummation for the production of gluino-gluino and squark-antisquark pairs at the LHC", *Phys. Rev. D* **80** (2009) 095004, doi:10.1103/PhysRevD.80.095004, arXiv:0905.4749.

[58] W. Beenakker et al., "Soft-gluon resummation for squark and gluino hadroproduction", *JHEP* **12** (2009) 041, doi:10.1088/1126-6708/2009/12/041, arXiv:0909.4418.

[59] W. Beenakker et al., "Squark and gluino hadroproduction", *Int. J. Mod. Phys. A* **26** (2011) 2637, doi:10.1142/S0217751X11053560, arXiv:1105.1110.

[60] CMS Collaboration, "Study of the underlying event at forward rapidity in pp collisions at $\sqrt{s}$ = 0.9, 2.76, and 7 TeV", *JHEP* **04** (2013) 072, doi:10.1007/JHEP04(2013)072, arXiv:1302.2394.

[61] R. Field, "Early LHC underlying event data: Findings and surprises", in *Hadron collider physics. Proceedings, 22nd Conference, HCP 2010, Toronto, Canada, August 23-27, 2010*. 2010. arXiv:1010.3558.

[62] CTEQ Collaboration, "Global QCD analysis of parton structure of the nucleon: CTEQ5 parton distributions", *Eur. Phys. J. C* **12** (2000) 375, doi:10.1007/s100529900196, arXiv:hep-ph/9903282.

[63] GEANT4 Collaboration, "GEANT4—a simulation toolkit", *Nucl. Instrum. Meth. A* **506** (2003) 250, doi:10.1016/S0168-9002(03)01368-8.

[64] CMS Collaboration, "The fast simulation of the CMS detector at LHC", *J. Phys. Conf. Ser.* **331** (2011) 032049, doi:10.1088/1742-6596/331/3/032049.

[65] CMS Collaboration, "Missing transverse energy performance of the CMS detector", *JINST* **6** (2011) P09001, doi:10.1088/1748-0221/6/09/P09001, arXiv:1106.5048.

[66] CMS Collaboration, "Performance of the CMS missing transverse momentum reconstruction in pp data at $\sqrt{s} = 8$ TeV", *JINST* **10** (2015) P02006, doi:10.1088/1748-0221/10/02/P02006, arXiv:1411.0511.

[67] CMS Collaboration, "Pileup removal algorithms", CMS Physics Analysis Summary CMS-PAS-JME-14-001, 2014.

[68] M. Cacciari and G. P. Salam, "Pileup subtraction using jet areas", *Phys. Lett. B* **659** (2008) 119, doi:10.1016/j.physletb.2007.09.077, arXiv:0707.1378.

[69] M. Cacciari, G. P. Salam, and G. Soyez, "The catchment area of jets", *JHEP* **04** (2008) 005, doi:10.1088/1126-6708/2008/04/005, arXiv:0802.1188.

[70] M. Cacciari, G. P. Salam, and G. Soyez, "FastJet user manual", *Eur. Phys. J. C* **72** (2012) 1896, doi:10.1140/epjc/s10052-012-1896-2, arXiv:1111.6097.

[71] M. Cacciari, G. P. Salam, and G. Soyez, "The anti-k_t jet clustering algorithm", *JHEP* **04** (2008) 063, doi:10.1088/1126-6708/2008/04/063, arXiv:0802.1189.

[72] CMS Collaboration, "Determination of jet energy calibration and transverse momentum resolution in CMS", *JINST* **6** (2011) P11002, doi:10.1088/1748-0221/6/11/P11002, arXiv:1107.4277.

[73] CMS Collaboration, "Identification of b-quark jets with the CMS experiment", *JINST* **8** (2013) P04013, doi:10.1088/1748-0221/8/04/P04013, arXiv:1211.4462.

[74] CMS Collaboration, "Performance of b tagging at $\sqrt{s} = 8$ TeV in multijet, $t\bar{t}$ and boosted topology events", CMS Physics Analysis Summary CMS-PAS-BTV-13-001, 2013.

[75] CMS Collaboration, "Search for massive resonances in dijet systems containing jets tagged as W or Z boson decays in pp collisions at $\sqrt{s} = 8\,\text{TeV}$", *JHEP* **08** (2014) 173, doi:10.1007/JHEP08(2014)173, arXiv:1405.1994.

[76] Y. L. Dokshitzer, G. D. Leder, S. Moretti, and B. R. Webber, "Better jet clustering algorithms", *JHEP* **08** (1997) 001, doi:10.1088/1126-6708/1997/08/001, arXiv:hep-ph/9707323.

[77] CMS Collaboration, "Performance of electron reconstruction and selection with the CMS detector in proton-proton collisions at $\sqrt{s} = 8\,\text{TeV}$", *JINST* **10** (2015) P06005, doi:10.1088/1748-0221/10/06/P06005, arXiv:1502.02701.

[78] CMS Collaboration, "Performance of CMS muon reconstruction in pp collision events at $\sqrt{s} = 7\,\text{TeV}$", *JINST* **7** (2012) P10002, doi:10.1088/1748-0221/7/10/P10002, arXiv:1206.4071.

[79] CMS Collaboration, "Identification techniques for highly boosted W bosons that decay into hadrons", *JHEP* **12** (2014) 017, doi:10.1007/JHEP12(2014)017, arXiv:1410.4227.

[80] T. Junk, "Confidence level computation for combining searches with small statistics", *Nucl. Instrum. Meth. A* **434** (1999) 435, doi:10.1016/S0168-9002(99)00498-2, arXiv:hep-ex/9902006.

[81] A. L. Read, "Presentation of search results: The CL_S technique", *J. Phys. G* **28** (2002) 2693, doi:10.1088/0954-3899/28/10/313.

[82] ATLAS and CMS Collaborations, "Procedure for the LHC Higgs boson search combination in Summer 2011", Technical Report CMS-NOTE-2011-005, ATL-PHYS-PUB-2011-11, 2011.

[83] NNPDF Collaboration, "Parton distributions with QED corrections", *Nucl. Phys. B* **877** (2013) 290, doi:10.1016/j.nuclphysb.2013.10.010, arXiv:1308.0598.

[84] A. D. Martin, W. J. Stirling, R. S. Thorne, and G. Watt, "Parton distributions for the LHC", *Eur. Phys. J. C* **63** (2009) 189, doi:10.1140/epjc/s10052-009-1072-5, arXiv:0901.0002.

[85] A. Buckley et al., "LHAPDF6: parton density access in the LHC precision era", *Eur. Phys. J. C* **75** (2015) 132, doi:10.1140/epjc/s10052-015-3318-8, arXiv:1412.7420.

[86] CMS Collaboration, "Measurement of differential top-quark pair production cross sections in pp collisions at $\sqrt{s} = 7\,\text{TeV}$", *Eur. Phys. J. C* **73** (2013) 2339, doi:10.1140/epjc/s10052-013-2339-4, arXiv:1211.2220.

12 The CMS Collaboration

Yerevan Physics Institute, Yerevan, Armenia
V. Khachatryan, A.M. Sirunyan, A. Tumasyan

Institut für Hochenergiephysik der OeAW, Wien, Austria
W. Adam, E. Asilar, T. Bergauer, J. Brandstetter, E. Brondolin, M. Dragicevic, J. Erö, M. Flechl, M. Friedl, R. Frühwirth[1], V.M. Ghete, C. Hartl, N. Hörmann, J. Hrubec, M. Jeitler[1], V. Knünz, A. König, M. Krammer[1], I. Krätschmer, D. Liko, T. Matsushita, I. Mikulec, D. Rabady[2], N. Rad, B. Rahbaran, H. Rohringer, J. Schieck[1], R. Schöfbeck, J. Strauss, W. Treberer-Treberspurg, W. Waltenberger, C.-E. Wulz[1]

National Centre for Particle and High Energy Physics, Minsk, Belarus
V. Mossolov, N. Shumeiko, J. Suarez Gonzalez

Universiteit Antwerpen, Antwerpen, Belgium
S. Alderweireldt, T. Cornelis, E.A. De Wolf, X. Janssen, A. Knutsson, J. Lauwers, S. Luyckx, M. Van De Klundert, H. Van Haevermaet, P. Van Mechelen, N. Van Remortel, A. Van Spilbeeck

Vrije Universiteit Brussel, Brussel, Belgium
S. Abu Zeid, F. Blekman, J. D'Hondt, N. Daci, I. De Bruyn, K. Deroover, N. Heracleous, J. Keaveney, S. Lowette, L. Moreels, A. Olbrechts, Q. Python, D. Strom, S. Tavernier, W. Van Doninck, P. Van Mulders, G.P. Van Onsem, I. Van Parijs

Université Libre de Bruxelles, Bruxelles, Belgium
P. Barria, H. Brun, C. Caillol, B. Clerbaux, G. De Lentdecker, W. Fang, G. Fasanella, L. Favart, R. Goldouzian, A. Grebenyuk, G. Karapostoli, T. Lenzi, A. Léonard, T. Maerschalk, A. Marinov, L. Perniè, A. Randle-conde, T. Seva, C. Vander Velde, P. Vanlaer, R. Yonamine, F. Zenoni, F. Zhang[3]

Ghent University, Ghent, Belgium
K. Beernaert, L. Benucci, A. Cimmino, S. Crucy, D. Dobur, A. Fagot, G. Garcia, M. Gul, J. Mccartin, A.A. Ocampo Rios, D. Poyraz, D. Ryckbosch, S. Salva, M. Sigamani, M. Tytgat, W. Van Driessche, E. Yazgan, N. Zaganidis

Université Catholique de Louvain, Louvain-la-Neuve, Belgium
S. Basegmez, C. Beluffi[4], O. Bondu, S. Brochet, G. Bruno, A. Caudron, L. Ceard, C. Delaere, M. Delcourt, D. Favart, L. Forthomme, A. Giammanco, A. Jafari, P. Jez, M. Komm, V. Lemaitre, A. Mertens, M. Musich, C. Nuttens, L. Perrini, K. Piotrzkowski, A. Popov[5], L. Quertenmont, M. Selvaggi, M. Vidal Marono

Université de Mons, Mons, Belgium
N. Beliy, G.H. Hammad

Centro Brasileiro de Pesquisas Fisicas, Rio de Janeiro, Brazil
W.L. Aldá Júnior, F.L. Alves, G.A. Alves, L. Brito, M. Correa Martins Junior, M. Hamer, C. Hensel, A. Moraes, M.E. Pol, P. Rebello Teles

Universidade do Estado do Rio de Janeiro, Rio de Janeiro, Brazil
E. Belchior Batista Das Chagas, W. Carvalho, J. Chinellato[6], A. Custódio, E.M. Da Costa, D. De Jesus Damiao, C. De Oliveira Martins, S. Fonseca De Souza, L.M. Huertas Guativa, H. Malbouisson, D. Matos Figueiredo, C. Mora Herrera, L. Mundim, H. Nogima, W.L. Prado Da Silva, A. Santoro, A. Sznajder, E.J. Tonelli Manganote[6], A. Vilela Pereira

Universidade Estadual Paulista [a], Universidade Federal do ABC [b], São Paulo, Brazil
S. Ahuja[a], C.A. Bernardes[b], A. De Souza Santos[b], S. Dogra[a], T.R. Fernandez Perez Tomei[a], E.M. Gregores[b], P.G. Mercadante[b], C.S. Moon[a,7], S.F. Novaes[a], Sandra S. Padula[a], D. Romero Abad[b], J.C. Ruiz Vargas

Institute for Nuclear Research and Nuclear Energy, Sofia, Bulgaria
A. Aleksandrov, R. Hadjiiska, P. Iaydjiev, M. Rodozov, S. Stoykova, G. Sultanov, M. Vutova

University of Sofia, Sofia, Bulgaria
A. Dimitrov, I. Glushkov, L. Litov, B. Pavlov, P. Petkov

Institute of High Energy Physics, Beijing, China
M. Ahmad, J.G. Bian, G.M. Chen, H.S. Chen, M. Chen, T. Cheng, R. Du, C.H. Jiang, D. Leggat, R. Plestina[8], F. Romeo, S.M. Shaheen, A. Spiezia, J. Tao, C. Wang, Z. Wang, H. Zhang

State Key Laboratory of Nuclear Physics and Technology, Peking University, Beijing, China
C. Asawatangtrakuldee, Y. Ban, Q. Li, S. Liu, Y. Mao, S.J. Qian, D. Wang, Z. Xu

Universidad de Los Andes, Bogota, Colombia
C. Avila, A. Cabrera, L.F. Chaparro Sierra, C. Florez, J.P. Gomez, B. Gomez Moreno, J.C. Sanabria

University of Split, Faculty of Electrical Engineering, Mechanical Engineering and Naval Architecture, Split, Croatia
N. Godinovic, D. Lelas, I. Puljak, P.M. Ribeiro Cipriano

University of Split, Faculty of Science, Split, Croatia
Z. Antunovic, M. Kovac

Institute Rudjer Boskovic, Zagreb, Croatia
V. Brigljevic, K. Kadija, J. Luetic, S. Micanovic, L. Sudic

University of Cyprus, Nicosia, Cyprus
A. Attikis, G. Mavromanolakis, J. Mousa, C. Nicolaou, F. Ptochos, P.A. Razis, H. Rykaczewski

Charles University, Prague, Czech Republic
M. Bodlak, M. Finger[9], M. Finger Jr.[9]

Academy of Scientific Research and Technology of the Arab Republic of Egypt, Egyptian Network of High Energy Physics, Cairo, Egypt
Y. Assran[10,11], S. Elgammal[10], A. Ellithi Kamel[12,12], M.A. Mahmoud[13,10]

National Institute of Chemical Physics and Biophysics, Tallinn, Estonia
B. Calpas, M. Kadastik, M. Murumaa, M. Raidal, A. Tiko, C. Veelken

Department of Physics, University of Helsinki, Helsinki, Finland
P. Eerola, J. Pekkanen, M. Voutilainen

Helsinki Institute of Physics, Helsinki, Finland
J. Härkönen, V. Karimäki, R. Kinnunen, T. Lampén, K. Lassila-Perini, S. Lehti, T. Lindén, P. Luukka, T. Peltola, J. Tuominiemi, E. Tuovinen, L. Wendland

Lappeenranta University of Technology, Lappeenranta, Finland
J. Talvitie, T. Tuuva

DSM/IRFU, CEA/Saclay, Gif-sur-Yvette, France
M. Besancon, F. Couderc, M. Dejardin, D. Denegri, B. Fabbro, J.L. Faure, C. Favaro, F. Ferri,

S. Ganjour, A. Givernaud, P. Gras, G. Hamel de Monchenault, P. Jarry, E. Locci, M. Machet, J. Malcles, J. Rander, A. Rosowsky, M. Titov, A. Zghiche

Laboratoire Leprince-Ringuet, Ecole Polytechnique, IN2P3-CNRS, Palaiseau, France
A. Abdulsalam, I. Antropov, S. Baffioni, F. Beaudette, P. Busson, L. Cadamuro, E. Chapon, C. Charlot, O. Davignon, N. Filipovic, R. Granier de Cassagnac, M. Jo, S. Lisniak, L. Mastrolorenzo, P. Miné, I.N. Naranjo, M. Nguyen, C. Ochando, G. Ortona, P. Paganini, P. Pigard, S. Regnard, R. Salerno, J.B. Sauvan, Y. Sirois, T. Strebler, Y. Yilmaz, A. Zabi

Institut Pluridisciplinaire Hubert Curien, Université de Strasbourg, Université de Haute Alsace Mulhouse, CNRS/IN2P3, Strasbourg, France
J.-L. Agram[14], J. Andrea, A. Aubin, D. Bloch, J.-M. Brom, M. Buttignol, E.C. Chabert, N. Chanon, C. Collard, E. Conte[14], X. Coubez, J.-C. Fontaine[14], D. Gelé, U. Goerlach, C. Goetzmann, A.-C. Le Bihan, J.A. Merlin[2], K. Skovpen, P. Van Hove

Centre de Calcul de l'Institut National de Physique Nucleaire et de Physique des Particules, CNRS/IN2P3, Villeurbanne, France
S. Gadrat

Université de Lyon, Université Claude Bernard Lyon 1, CNRS-IN2P3, Institut de Physique Nucléaire de Lyon, Villeurbanne, France
S. Beauceron, C. Bernet, G. Boudoul, E. Bouvier, C.A. Carrillo Montoya, R. Chierici, D. Contardo, B. Courbon, P. Depasse, H. El Mamouni, J. Fan, J. Fay, S. Gascon, M. Gouzevitch, B. Ille, F. Lagarde, I.B. Laktineh, M. Lethuillier, L. Mirabito, A.L. Pequegnot, S. Perries, J.D. Ruiz Alvarez, D. Sabes, V. Sordini, M. Vander Donckt, P. Verdier, S. Viret

Georgian Technical University, Tbilisi, Georgia
T. Toriashvili[15]

Tbilisi State University, Tbilisi, Georgia
Z. Tsamalaidze[9]

RWTH Aachen University, I. Physikalisches Institut, Aachen, Germany
C. Autermann, S. Beranek, L. Feld, A. Heister, M.K. Kiesel, K. Klein, M. Lipinski, A. Ostapchuk, M. Preuten, F. Raupach, S. Schael, J.F. Schulte, T. Verlage, H. Weber, V. Zhukov[5]

RWTH Aachen University, III. Physikalisches Institut A, Aachen, Germany
M. Ata, M. Brodski, E. Dietz-Laursonn, D. Duchardt, M. Endres, M. Erdmann, S. Erdweg, T. Esch, R. Fischer, A. Güth, T. Hebbeker, C. Heidemann, K. Hoepfner, S. Knutzen, P. Kreuzer, M. Merschmeyer, A. Meyer, P. Millet, S. Mukherjee, M. Olschewski, K. Padeken, P. Papacz, T. Pook, M. Radziej, H. Reithler, M. Rieger, F. Scheuch, L. Sonnenschein, D. Teyssier, S. Thüer

RWTH Aachen University, III. Physikalisches Institut B, Aachen, Germany
V. Cherepanov, Y. Erdogan, G. Flügge, H. Geenen, M. Geisler, F. Hoehle, B. Kargoll, T. Kress, A. Künsken, J. Lingemann, A. Nehrkorn, A. Nowack, I.M. Nugent, C. Pistone, O. Pooth, A. Stahl

Deutsches Elektronen-Synchrotron, Hamburg, Germany
M. Aldaya Martin, I. Asin, N. Bartosik, O. Behnke, U. Behrens, K. Borras[16], A. Burgmeier, A. Campbell, C. Contreras-Campana, F. Costanza, C. Diez Pardos, G. Dolinska, S. Dooling, T. Dorland, G. Eckerlin, D. Eckstein, T. Eichhorn, G. Flucke, E. Gallo[17], J. Garay Garcia, A. Geiser, A. Gizhko, P. Gunnellini, J. Hauk, M. Hempel[18], H. Jung, A. Kalogeropoulos, O. Karacheban[18], M. Kasemann, P. Katsas, J. Kieseler, C. Kleinwort, I. Korol, W. Lange, J. Leonard, K. Lipka, A. Lobanov, W. Lohmann[18], R. Mankel, I.-A. Melzer-Pellmann,

A.B. Meyer, G. Mittag, J. Mnich, A. Mussgiller, S. Naumann-Emme, A. Nayak, E. Ntomari, H. Perrey, D. Pitzl, R. Placakyte, A. Raspereza, B. Roland, M.Ö. Sahin, P. Saxena, T. Schoerner-Sadenius, C. Seitz, S. Spannagel, N. Stefaniuk, K.D. Trippkewitz, R. Walsh, C. Wissing

University of Hamburg, Hamburg, Germany
V. Blobel, M. Centis Vignali, A.R. Draeger, J. Erfle, E. Garutti, K. Goebel, D. Gonzalez, M. Görner, J. Haller, M. Hoffmann, R.S. Höing, A. Junkes, R. Klanner, R. Kogler, N. Kovalchuk, T. Lapsien, T. Lenz, I. Marchesini, D. Marconi, M. Meyer, D. Nowatschin, J. Ott, F. Pantaleo[2], T. Peiffer, A. Perieanu, N. Pietsch, J. Poehlsen, D. Rathjens, C. Sander, C. Scharf, P. Schleper, E. Schlieckau, A. Schmidt, S. Schumann, J. Schwandt, V. Sola, H. Stadie, G. Steinbrück, F.M. Stober, H. Tholen, D. Troendle, E. Usai, L. Vanelderen, A. Vanhoefer, B. Vormwald

Institut für Experimentelle Kernphysik, Karlsruhe, Germany
C. Barth, C. Baus, J. Berger, C. Böser, E. Butz, T. Chwalek, F. Colombo, W. De Boer, A. Descroix, A. Dierlamm, S. Fink, F. Frensch, R. Friese, M. Giffels, A. Gilbert, D. Haitz, F. Hartmann[2], S.M. Heindl, U. Husemann, I. Katkov[5], A. Kornmayer[2], P. Lobelle Pardo, B. Maier, H. Mildner, M.U. Mozer, T. Müller, Th. Müller, M. Plagge, G. Quast, K. Rabbertz, S. Röcker, F. Roscher, M. Schröder, G. Sieber, H.J. Simonis, R. Ulrich, J. Wagner-Kuhr, S. Wayand, M. Weber, T. Weiler, S. Williamson, C. Wöhrmann, R. Wolf

Institute of Nuclear and Particle Physics (INPP), NCSR Demokritos, Aghia Paraskevi, Greece
G. Anagnostou, G. Daskalakis, T. Geralis, V.A. Giakoumopoulou, A. Kyriakis, D. Loukas, A. Psallidas, I. Topsis-Giotis

National and Kapodistrian University of Athens, Athens, Greece
A. Agapitos, S. Kesisoglou, A. Panagiotou, N. Saoulidou, E. Tziaferi

University of Ioánnina, Ioánnina, Greece
I. Evangelou, G. Flouris, C. Foudas, P. Kokkas, N. Loukas, N. Manthos, I. Papadopoulos, E. Paradas, J. Strologas

Wigner Research Centre for Physics, Budapest, Hungary
G. Bencze, C. Hajdu, A. Hazi, P. Hidas, D. Horvath[19], F. Sikler, V. Veszpremi, G. Vesztergombi[20], A.J. Zsigmond

Institute of Nuclear Research ATOMKI, Debrecen, Hungary
N. Beni, S. Czellar, J. Karancsi[21], J. Molnar, Z. Szillasi[2]

University of Debrecen, Debrecen, Hungary
M. Bartók[22], A. Makovec, P. Raics, Z.L. Trocsanyi, B. Ujvari

National Institute of Science Education and Research, Bhubaneswar, India
S. Choudhury[23], P. Mal, K. Mandal, D.K. Sahoo, N. Sahoo, S.K. Swain

Panjab University, Chandigarh, India
S. Bansal, S.B. Beri, V. Bhatnagar, R. Chawla, R. Gupta, U.Bhawandeep, A.K. Kalsi, A. Kaur, M. Kaur, R. Kumar, A. Mehta, M. Mittal, J.B. Singh, G. Walia

University of Delhi, Delhi, India
Ashok Kumar, A. Bhardwaj, B.C. Choudhary, R.B. Garg, S. Malhotra, M. Naimuddin, N. Nishu, K. Ranjan, R. Sharma, V. Sharma

Saha Institute of Nuclear Physics, Kolkata, India
S. Bhattacharya, K. Chatterjee, S. Dey, S. Dutta, N. Majumdar, A. Modak, K. Mondal, S. Mukhopadhyay, A. Roy, D. Roy, S. Roy Chowdhury, S. Sarkar, M. Sharan

Bhabha Atomic Research Centre, Mumbai, India
R. Chudasama, D. Dutta, V. Jha, V. Kumar, A.K. Mohanty[2], L.M. Pant, P. Shukla, A. Topkar

Tata Institute of Fundamental Research, Mumbai, India
T. Aziz, S. Banerjee, S. Bhowmik[24], R.M. Chatterjee, R.K. Dewanjee, S. Dugad, S. Ganguly, S. Ghosh, M. Guchait, A. Gurtu[25], Sa. Jain, G. Kole, S. Kumar, B. Mahakud, M. Maity[24], G. Majumder, K. Mazumdar, S. Mitra, G.B. Mohanty, B. Parida, T. Sarkar[24], N. Sur, B. Sutar, N. Wickramage[26]

Indian Institute of Science Education and Research (IISER), Pune, India
S. Chauhan, S. Dube, A. Kapoor, K. Kothekar, S. Sharma

Institute for Research in Fundamental Sciences (IPM), Tehran, Iran
H. Bakhshiansohi, H. Behnamian, S.M. Etesami[27], A. Fahim[28], M. Khakzad, M. Mohammadi Najafabadi, M. Naseri, S. Paktinat Mehdiabadi, F. Rezaei Hosseinabadi, B. Safarzadeh[29], M. Zeinali

University College Dublin, Dublin, Ireland
M. Felcini, M. Grunewald

INFN Sezione di Bari [a], Università di Bari [b], Politecnico di Bari [c], Bari, Italy
M. Abbrescia[a,b], C. Calabria[a,b], C. Caputo[a,b], A. Colaleo[a], D. Creanza[a,c], L. Cristella[a,b], N. De Filippis[a,c], M. De Palma[a,b], L. Fiore[a], G. Iaselli[a,c], G. Maggi[a,c], M. Maggi[a], G. Miniello[a,b], S. My[a,c], S. Nuzzo[a,b], A. Pompili[a,b], G. Pugliese[a,c], R. Radogna[a,b], A. Ranieri[a], G. Selvaggi[a,b], L. Silvestris[a,2], R. Venditti[a,b]

INFN Sezione di Bologna [a], Università di Bologna [b], Bologna, Italy
G. Abbiendi[a], C. Battilana[2], D. Bonacorsi[a,b], S. Braibant-Giacomelli[a,b], L. Brigliadori[a,b], R. Campanini[a,b], P. Capiluppi[a,b], A. Castro[a,b], F.R. Cavallo[a], S.S. Chhibra[a,b], G. Codispoti[a,b], M. Cuffiani[a,b], G.M. Dallavalle[a], F. Fabbri[a], A. Fanfani[a,b], D. Fasanella[a,b], P. Giacomelli[a], C. Grandi[a], L. Guiducci[a,b], S. Marcellini[a], G. Masetti[a], A. Montanari[a], F.L. Navarria[a,b], A. Perrotta[a], A.M. Rossi[a,b], T. Rovelli[a,b], G.P. Siroli[a,b], N. Tosi[a,b,2]

INFN Sezione di Catania [a], Università di Catania [b], Catania, Italy
G. Cappello[b], M. Chiorboli[a,b], S. Costa[a,b], A. Di Mattia[a], F. Giordano[a,b], R. Potenza[a,b], A. Tricomi[a,b], C. Tuve[a,b]

INFN Sezione di Firenze [a], Università di Firenze [b], Firenze, Italy
G. Barbagli[a], V. Ciulli[a,b], C. Civinini[a], R. D'Alessandro[a,b], E. Focardi[a,b], V. Gori[a,b], P. Lenzi[a,b], M. Meschini[a], S. Paoletti[a], G. Sguazzoni[a], L. Viliani[a,b,2]

INFN Laboratori Nazionali di Frascati, Frascati, Italy
L. Benussi, S. Bianco, F. Fabbri, D. Piccolo, F. Primavera[2]

INFN Sezione di Genova [a], Università di Genova [b], Genova, Italy
V. Calvelli[a,b], F. Ferro[a], M. Lo Vetere[a,b], M.R. Monge[a,b], E. Robutti[a], S. Tosi[a,b]

INFN Sezione di Milano-Bicocca [a], Università di Milano-Bicocca [b], Milano, Italy
L. Brianza, M.E. Dinardo[a,b], S. Fiorendi[a,b], S. Gennai[a], R. Gerosa[a,b], A. Ghezzi[a,b], P. Govoni[a,b], S. Malvezzi[a], R.A. Manzoni[a,b,2], B. Marzocchi[a,b], D. Menasce[a], L. Moroni[a], M. Paganoni[a,b], D. Pedrini[a], S. Ragazzi[a,b], N. Redaelli[a], T. Tabarelli de Fatis[a,b]

INFN Sezione di Napoli [a], Università di Napoli 'Federico II' [b], Napoli, Italy, Università della Basilicata [c], Potenza, Italy, Università G. Marconi [d], Roma, Italy
S. Buontempo[a], N. Cavallo[a,c], S. Di Guida[a,d,2], M. Esposito[a,b], F. Fabozzi[a,c], A.O.M. Iorio[a,b], G. Lanza[a], L. Lista[a], S. Meola[a,d,2], M. Merola[a], P. Paolucci[a,2], C. Sciacca[a,b], F. Thyssen

INFN Sezione di Padova [a], Università di Padova [b], Padova, Italy, Università di Trento [c], Trento, Italy
P. Azzi[a,2], N. Bacchetta[a], L. Benato[a,b], D. Bisello[a,b], A. Boletti[a,b], R. Carlin[a,b], P. Checchia[a], M. Dall'Osso[a,b,2], T. Dorigo[a], U. Dosselli[a], F. Gasparini[a,b], U. Gasparini[a,b], F. Gonella[a], A. Gozzelino[a], M. Gulmini[a,30], S. Lacaprara[a], M. Margoni[a,b], A.T. Meneguzzo[a,b], F. Montecassiano[a], J. Pazzini[a,b,2], N. Pozzobon[a,b], P. Ronchese[a,b], F. Simonetto[a,b], E. Torassa[a], M. Tosi[a,b], M. Zanetti, P. Zotto[a,b], A. Zucchetta[a,b,2], G. Zumerle[a,b]

INFN Sezione di Pavia [a], Università di Pavia [b], Pavia, Italy
A. Braghieri[a], A. Magnani[a,b], P. Montagna[a,b], S.P. Ratti[a,b], V. Re[a], C. Riccardi[a,b], P. Salvini[a], I. Vai[a,b], P. Vitulo[a,b]

INFN Sezione di Perugia [a], Università di Perugia [b], Perugia, Italy
L. Alunni Solestizi[a,b], G.M. Bilei[a], D. Ciangottini[a,b,2], L. Fanò[a,b], P. Lariccia[a,b], G. Mantovani[a,b], M. Menichelli[a], A. Saha[a], A. Santocchia[a,b]

INFN Sezione di Pisa [a], Università di Pisa [b], Scuola Normale Superiore di Pisa [c], Pisa, Italy
K. Androsov[a,31], P. Azzurri[a,2], G. Bagliesi[a], J. Bernardini[a], T. Boccali[a], R. Castaldi[a], M.A. Ciocci[a,31], R. Dell'Orso[a], S. Donato[a,c,2], G. Fedi, L. Foà[a,c†], A. Giassi[a], M.T. Grippo[a,31], F. Ligabue[a,c], T. Lomtadze[a], L. Martini[a,b], A. Messineo[a,b], F. Palla[a], A. Rizzi[a,b], A. Savoy-Navarro[a,32], A.T. Serban[a], P. Spagnolo[a], R. Tenchini[a], G. Tonelli[a,b], A. Venturi[a], P.G. Verdini[a]

INFN Sezione di Roma [a], Università di Roma [b], Roma, Italy
L. Barone[a,b], F. Cavallari[a], G. D'imperio[a,b,2], D. Del Re[a,b,2], M. Diemoz[a], S. Gelli[a,b], C. Jorda[a], E. Longo[a,b], F. Margaroli[a,b], P. Meridiani[a], G. Organtini[a,b], R. Paramatti[a], F. Preiato[a,b], S. Rahatlou[a,b], C. Rovelli[a], F. Santanastasio[a,b], P. Traczyk[a,b,2]

INFN Sezione di Torino [a], Università di Torino [b], Torino, Italy, Università del Piemonte Orientale [c], Novara, Italy
N. Amapane[a,b], R. Arcidiacono[a,c,2], S. Argiro[a,b], M. Arneodo[a,c], R. Bellan[a,b], C. Biino[a], N. Cartiglia[a], M. Costa[a,b], R. Covarelli[a,b], A. Degano[a,b], N. Demaria[a], L. Finco[a,b,2], B. Kiani[a,b], C. Mariotti[a], S. Maselli[a], E. Migliore[a,b], V. Monaco[a,b], E. Monteil[a,b], M.M. Obertino[a,b], L. Pacher[a,b], N. Pastrone[a], M. Pelliccioni[a], G.L. Pinna Angioni[a,b], F. Ravera[a,b], A. Romero[a,b], M. Ruspa[a,c], R. Sacchi[a,b], A. Solano[a,b], A. Staiano[a]

INFN Sezione di Trieste [a], Università di Trieste [b], Trieste, Italy
S. Belforte[a], V. Candelise[a,b], M. Casarsa[a], F. Cossutti[a], G. Della Ricca[a,b], B. Gobbo[a], C. La Licata[a,b], M. Marone[a,b], A. Schizzi[a,b], A. Zanetti[a]

Kangwon National University, Chunchon, Korea
A. Kropivnitskaya, S.K. Nam

Kyungpook National University, Daegu, Korea
D.H. Kim, G.N. Kim, M.S. Kim, D.J. Kong, S. Lee, Y.D. Oh, A. Sakharov, S. Sekmen, D.C. Son

Chonbuk National University, Jeonju, Korea
J.A. Brochero Cifuentes, H. Kim, T.J. Kim

Chonnam National University, Institute for Universe and Elementary Particles, Kwangju, Korea
S. Song

Korea University, Seoul, Korea
S. Cho, S. Choi, Y. Go, D. Gyun, B. Hong, H. Kim, Y. Kim, B. Lee, K. Lee, K.S. Lee, S. Lee, J. Lim, S.K. Park, Y. Roh

Seoul National University, Seoul, Korea
H.D. Yoo

University of Seoul, Seoul, Korea
M. Choi, H. Kim, J.H. Kim, J.S.H. Lee, I.C. Park, G. Ryu, M.S. Ryu

Sungkyunkwan University, Suwon, Korea
Y. Choi, J. Goh, D. Kim, E. Kwon, J. Lee, I. Yu

Vilnius University, Vilnius, Lithuania
V. Dudenas, A. Juodagalvis, J. Vaitkus

National Centre for Particle Physics, Universiti Malaya, Kuala Lumpur, Malaysia
I. Ahmed, Z.A. Ibrahim, J.R. Komaragiri, M.A.B. Md Ali[33], F. Mohamad Idris[34], W.A.T. Wan Abdullah, M.N. Yusli, Z. Zolkapli

Centro de Investigacion y de Estudios Avanzados del IPN, Mexico City, Mexico
E. Casimiro Linares, H. Castilla-Valdez, E. De La Cruz-Burelo, I. Heredia-De La Cruz[35], A. Hernandez-Almada, R. Lopez-Fernandez, J. Mejia Guisao, A. Sanchez-Hernandez

Universidad Iberoamericana, Mexico City, Mexico
S. Carrillo Moreno, F. Vazquez Valencia

Benemerita Universidad Autonoma de Puebla, Puebla, Mexico
I. Pedraza, H.A. Salazar Ibarguen

Universidad Autónoma de San Luis Potosí, San Luis Potosí, Mexico
A. Morelos Pineda

University of Auckland, Auckland, New Zealand
D. Krofcheck

University of Canterbury, Christchurch, New Zealand
P.H. Butler

National Centre for Physics, Quaid-I-Azam University, Islamabad, Pakistan
A. Ahmad, M. Ahmad, Q. Hassan, H.R. Hoorani, W.A. Khan, T. Khurshid, M. Shoaib, M. Waqas

National Centre for Nuclear Research, Swierk, Poland
H. Bialkowska, M. Bluj, B. Boimska, T. Frueboes, M. Górski, M. Kazana, K. Nawrocki, K. Romanowska-Rybinska, M. Szleper, P. Zalewski

Institute of Experimental Physics, Faculty of Physics, University of Warsaw, Warsaw, Poland
G. Brona, K. Bunkowski, A. Byszuk[36], K. Doroba, A. Kalinowski, M. Konecki, J. Krolikowski, M. Misiura, M. Olszewski, M. Walczak

Laboratório de Instrumentação e Física Experimental de Partículas, Lisboa, Portugal
P. Bargassa, C. Beirão Da Cruz E Silva, A. Di Francesco, P. Faccioli, P.G. Ferreira Parracho,

M. Gallinaro, J. Hollar, N. Leonardo, L. Lloret Iglesias, F. Nguyen, J. Rodrigues Antunes, J. Seixas, O. Toldaiev, D. Vadruccio, J. Varela, P. Vischia

Joint Institute for Nuclear Research, Dubna, Russia
S. Afanasiev, P. Bunin, M. Gavrilenko, I. Golutvin, I. Gorbunov, A. Kamenev, V. Karjavin, A. Lanev, A. Malakhov, V. Matveev[37,38], P. Moisenz, V. Palichik, V. Perelygin, S. Shmatov, S. Shulha, N. Skatchkov, V. Smirnov, A. Zarubin

Petersburg Nuclear Physics Institute, Gatchina (St. Petersburg), Russia
V. Golovtsov, Y. Ivanov, V. Kim[39], E. Kuznetsova, P. Levchenko, V. Murzin, V. Oreshkin, I. Smirnov, V. Sulimov, L. Uvarov, S. Vavilov, A. Vorobyev

Institute for Nuclear Research, Moscow, Russia
Yu. Andreev, A. Dermenev, S. Gninenko, N. Golubev, A. Karneyeu, M. Kirsanov, N. Krasnikov, A. Pashenkov, D. Tlisov, A. Toropin

Institute for Theoretical and Experimental Physics, Moscow, Russia
V. Epshteyn, V. Gavrilov, N. Lychkovskaya, V. Popov, I. Pozdnyakov, G. Safronov, A. Spiridonov, E. Vlasov, A. Zhokin

National Research Nuclear University 'Moscow Engineering Physics Institute' (MEPhI), Moscow, Russia
M. Chadeeva, R. Chistov, M. Danilov, V. Rusinov, E. Tarkovskii

P.N. Lebedev Physical Institute, Moscow, Russia
V. Andreev, M. Azarkin[38], I. Dremin[38], M. Kirakosyan, A. Leonidov[38], G. Mesyats, S.V. Rusakov

Skobeltsyn Institute of Nuclear Physics, Lomonosov Moscow State University, Moscow, Russia
A. Baskakov, A. Belyaev, E. Boos, M. Dubinin[40], L. Dudko, A. Ershov, A. Gribushin, V. Klyukhin, O. Kodolova, I. Lokhtin, I. Miagkov, S. Obraztsov, S. Petrushanko, V. Savrin, A. Snigirev

State Research Center of Russian Federation, Institute for High Energy Physics, Protvino, Russia
I. Azhgirey, I. Bayshev, S. Bitioukov, V. Kachanov, A. Kalinin, D. Konstantinov, V. Krychkine, V. Petrov, R. Ryutin, A. Sobol, L. Tourtchanovitch, S. Troshin, N. Tyurin, A. Uzunian, A. Volkov

University of Belgrade, Faculty of Physics and Vinca Institute of Nuclear Sciences, Belgrade, Serbia
P. Adzic[41], P. Cirkovic, D. Devetak, J. Milosevic, V. Rekovic

Centro de Investigaciones Energéticas Medioambientales y Tecnológicas (CIEMAT), Madrid, Spain
J. Alcaraz Maestre, E. Calvo, M. Cerrada, M. Chamizo Llatas, N. Colino, B. De La Cruz, A. Delgado Peris, A. Escalante Del Valle, C. Fernandez Bedoya, J.P. Fernández Ramos, J. Flix, M.C. Fouz, P. Garcia-Abia, O. Gonzalez Lopez, S. Goy Lopez, J.M. Hernandez, M.I. Josa, E. Navarro De Martino, A. Pérez-Calero Yzquierdo, J. Puerta Pelayo, A. Quintario Olmeda, I. Redondo, L. Romero, M.S. Soares

Universidad Autónoma de Madrid, Madrid, Spain
C. Albajar, J.F. de Trocóniz, M. Missiroli, D. Moran

Universidad de Oviedo, Oviedo, Spain
J. Cuevas, J. Fernandez Menendez, S. Folgueras, I. Gonzalez Caballero, E. Palencia Cortezon, J.M. Vizan Garcia

Instituto de Física de Cantabria (IFCA), CSIC-Universidad de Cantabria, Santander, Spain
I.J. Cabrillo, A. Calderon, J.R. Castiñeiras De Saa, E. Curras, P. De Castro Manzano, M. Fernandez, J. Garcia-Ferrero, G. Gomez, A. Lopez Virto, J. Marco, R. Marco, C. Martinez Rivero, F. Matorras, J. Piedra Gomez, T. Rodrigo, A.Y. Rodríguez-Marrero, A. Ruiz-Jimeno, L. Scodellaro, N. Trevisani, I. Vila, R. Vilar Cortabitarte

CERN, European Organization for Nuclear Research, Geneva, Switzerland
D. Abbaneo, E. Auffray, G. Auzinger, M. Bachtis, P. Baillon, A.H. Ball, D. Barney, A. Benaglia, J. Bendavid, L. Benhabib, G.M. Berruti, P. Bloch, A. Bocci, A. Bonato, C. Botta, H. Breuker, T. Camporesi, R. Castello, M. Cepeda, G. Cerminara, M. D'Alfonso, D. d'Enterria, A. Dabrowski, V. Daponte, A. David, M. De Gruttola, F. De Guio, A. De Roeck, S. De Visscher, E. Di Marco[42], M. Dobson, M. Dordevic, B. Dorney, T. du Pree, D. Duggan, M. Dünser, N. Dupont, A. Elliott-Peisert, G. Franzoni, J. Fulcher, W. Funk, D. Gigi, K. Gill, D. Giordano, M. Girone, F. Glege, R. Guida, S. Gundacker, M. Guthoff, J. Hammer, P. Harris, J. Hegeman, V. Innocente, P. Janot, H. Kirschenmann, M.J. Kortelainen, K. Kousouris, K. Krajczar, P. Lecoq, C. Lourenço, M.T. Lucchini, N. Magini, L. Malgeri, M. Mannelli, A. Martelli, L. Masetti, F. Meijers, S. Mersi, E. Meschi, F. Moortgat, S. Morovic, M. Mulders, M.V. Nemallapudi, H. Neugebauer, S. Orfanelli[43], L. Orsini, L. Pape, E. Perez, M. Peruzzi, A. Petrilli, G. Petrucciani, A. Pfeiffer, M. Pierini, D. Piparo, A. Racz, T. Reis, G. Rolandi[44], M. Rovere, M. Ruan, H. Sakulin, C. Schäfer, C. Schwick, M. Seidel, A. Sharma, P. Silva, M. Simon, P. Sphicas[45], J. Steggemann, B. Stieger, M. Stoye, Y. Takahashi, D. Treille, A. Triossi, A. Tsirou, G.I. Veres[20], N. Wardle, H.K. Wöhri, A. Zagozdzinska[36], W.D. Zeuner

Paul Scherrer Institut, Villigen, Switzerland
W. Bertl, K. Deiters, W. Erdmann, R. Horisberger, Q. Ingram, H.C. Kaestli, D. Kotlinski, U. Langenegger, T. Rohe

Institute for Particle Physics, ETH Zurich, Zurich, Switzerland
F. Bachmair, L. Bäni, L. Bianchini, B. Casal, G. Dissertori, M. Dittmar, M. Donegà, P. Eller, C. Grab, C. Heidegger, D. Hits, J. Hoss, G. Kasieczka, P. Lecomte[†], W. Lustermann, B. Mangano, M. Marionneau, P. Martinez Ruiz del Arbol, M. Masciovecchio, M.T. Meinhard, D. Meister, F. Micheli, P. Musella, F. Nessi-Tedaldi, F. Pandolfi, J. Pata, F. Pauss, G. Perrin, L. Perrozzi, M. Quittnat, M. Rossini, M. Schönenberger, A. Starodumov[46], M. Takahashi, V.R. Tavolaro, K. Theofilatos, R. Wallny

Universität Zürich, Zurich, Switzerland
T.K. Aarrestad, C. Amsler[47], L. Caminada, M.F. Canelli, V. Chiochia, A. De Cosa, C. Galloni, A. Hinzmann, T. Hreus, B. Kilminster, C. Lange, J. Ngadiuba, D. Pinna, G. Rauco, P. Robmann, D. Salerno, Y. Yang

National Central University, Chung-Li, Taiwan
K.H. Chen, T.H. Doan, Sh. Jain, R. Khurana, M. Konyushikhin, C.M. Kuo, W. Lin, Y.J. Lu, A. Pozdnyakov, S.S. Yu

National Taiwan University (NTU), Taipei, Taiwan
Arun Kumar, P. Chang, Y.H. Chang, Y.W. Chang, Y. Chao, K.F. Chen, P.H. Chen, C. Dietz, F. Fiori, U. Grundler, W.-S. Hou, Y. Hsiung, Y.F. Liu, R.-S. Lu, M. Miñano Moya, E. Petrakou, J.f. Tsai, Y.M. Tzeng

Chulalongkorn University, Faculty of Science, Department of Physics, Bangkok, Thailand
B. Asavapibhop, K. Kovitanggoon, G. Singh, N. Srimanobhas, N. Suwonjandee

Cukurova University, Adana, Turkey
A. Adiguzel, S. Cerci[48], S. Damarseckin, Z.S. Demiroglu, C. Dozen, I. Dumanoglu, E. Eskut, S. Girgis, G. Gokbulut, Y. Guler, E. Gurpinar, I. Hos, E.E. Kangal[49], A. Kayis Topaksu, G. Onengut[50], K. Ozdemir[51], S. Ozturk[52], A. Polatoz, C. Zorbilmez

Middle East Technical University, Physics Department, Ankara, Turkey
B. Bilin, S. Bilmis, B. Isildak[53], G. Karapinar[54], M. Yalvac, M. Zeyrek

Bogazici University, Istanbul, Turkey
E. Gülmez, M. Kaya[55], O. Kaya[56], E.A. Yetkin[57], T. Yetkin[58]

Istanbul Technical University, Istanbul, Turkey
A. Cakir, K. Cankocak, S. Sen[59], F.I. Vardarlı

Institute for Scintillation Materials of National Academy of Science of Ukraine, Kharkov, Ukraine
B. Grynyov

National Scientific Center, Kharkov Institute of Physics and Technology, Kharkov, Ukraine
L. Levchuk, P. Sorokin

University of Bristol, Bristol, United Kingdom
R. Aggleton, F. Ball, L. Beck, J.J. Brooke, D. Burns, E. Clement, D. Cussans, H. Flacher, J. Goldstein, M. Grimes, G.P. Heath, H.F. Heath, J. Jacob, L. Kreczko, C. Lucas, Z. Meng, D.M. Newbold[60], S. Paramesvaran, A. Poll, T. Sakuma, S. Seif El Nasr-storey, S. Senkin, D. Smith, V.J. Smith

Rutherford Appleton Laboratory, Didcot, United Kingdom
K.W. Bell, A. Belyaev[61], C. Brew, R.M. Brown, L. Calligaris, D. Cieri, D.J.A. Cockerill, J.A. Coughlan, K. Harder, S. Harper, E. Olaiya, D. Petyt, C.H. Shepherd-Themistocleous, A. Thea, I.R. Tomalin, T. Williams, S.D. Worm

Imperial College, London, United Kingdom
M. Baber, R. Bainbridge, O. Buchmuller, A. Bundock, D. Burton, S. Casasso, M. Citron, D. Colling, L. Corpe, P. Dauncey, G. Davies, A. De Wit, M. Della Negra, P. Dunne, A. Elwood, D. Futyan, G. Hall, G. Iles, R. Lane, R. Lucas[60], L. Lyons, A.-M. Magnan, S. Malik, J. Nash, A. Nikitenko[46], J. Pela, M. Pesaresi, D.M. Raymond, A. Richards, A. Rose, C. Seez, A. Tapper, K. Uchida, M. Vazquez Acosta[62], T. Virdee, S.C. Zenz

Brunel University, Uxbridge, United Kingdom
J.E. Cole, P.R. Hobson, A. Khan, P. Kyberd, D. Leslie, I.D. Reid, P. Symonds, L. Teodorescu, M. Turner

Baylor University, Waco, USA
A. Borzou, K. Call, J. Dittmann, K. Hatakeyama, H. Liu, N. Pastika

The University of Alabama, Tuscaloosa, USA
O. Charaf, S.I. Cooper, C. Henderson, P. Rumerio

Boston University, Boston, USA
D. Arcaro, A. Avetisyan, T. Bose, D. Gastler, D. Rankin, C. Richardson, J. Rohlf, L. Sulak, D. Zou

Brown University, Providence, USA
J. Alimena, G. Benelli, E. Berry, D. Cutts, A. Ferapontov, A. Garabedian, J. Hakala, U. Heintz, O. Jesus, E. Laird, G. Landsberg, Z. Mao, M. Narain, S. Piperov, S. Sagir, R. Syarif

University of California, Davis, Davis, USA
R. Breedon, G. Breto, M. Calderon De La Barca Sanchez, S. Chauhan, M. Chertok, J. Conway, R. Conway, P.T. Cox, R. Erbacher, G. Funk, M. Gardner, W. Ko, R. Lander, C. Mclean, M. Mulhearn, D. Pellett, J. Pilot, F. Ricci-Tam, S. Shalhout, J. Smith, M. Squires, D. Stolp, M. Tripathi, S. Wilbur, R. Yohay

University of California, Los Angeles, USA
R. Cousins, P. Everaerts, A. Florent, J. Hauser, M. Ignatenko, D. Saltzberg, E. Takasugi, V. Valuev, M. Weber

University of California, Riverside, Riverside, USA
K. Burt, R. Clare, J. Ellison, J.W. Gary, G. Hanson, J. Heilman, M. Ivova PANEVA, P. Jandir, E. Kennedy, F. Lacroix, O.R. Long, M. Malberti, M. Olmedo Negrete, A. Shrinivas, H. Wei, S. Wimpenny, B. R. Yates

University of California, San Diego, La Jolla, USA
J.G. Branson, G.B. Cerati, S. Cittolin, R.T. D'Agnolo, M. Derdzinski, A. Holzner, R. Kelley, D. Klein, J. Letts, I. Macneill, D. Olivito, S. Padhi, M. Pieri, M. Sani, V. Sharma, S. Simon, M. Tadel, A. Vartak, S. Wasserbaech[63], C. Welke, F. Würthwein, A. Yagil, G. Zevi Della Porta

University of California, Santa Barbara, Santa Barbara, USA
J. Bradmiller-Feld, C. Campagnari, A. Dishaw, V. Dutta, K. Flowers, M. Franco Sevilla, P. Geffert, C. George, F. Golf, L. Gouskos, J. Gran, J. Incandela, N. Mccoll, S.D. Mullin, J. Richman, D. Stuart, I. Suarez, C. West, J. Yoo

California Institute of Technology, Pasadena, USA
D. Anderson, A. Apresyan, A. Bornheim, J. Bunn, Y. Chen, J. Duarte, A. Mott, H.B. Newman, C. Pena, M. Spiropulu, J.R. Vlimant, S. Xie, R.Y. Zhu

Carnegie Mellon University, Pittsburgh, USA
M.B. Andrews, V. Azzolini, A. Calamba, B. Carlson, T. Ferguson, M. Paulini, J. Russ, M. Sun, H. Vogel, I. Vorobiev

University of Colorado Boulder, Boulder, USA
J.P. Cumalat, W.T. Ford, A. Gaz, F. Jensen, A. Johnson, M. Krohn, T. Mulholland, U. Nauenberg, K. Stenson, S.R. Wagner

Cornell University, Ithaca, USA
J. Alexander, A. Chatterjee, J. Chaves, J. Chu, S. Dittmer, N. Eggert, N. Mirman, G. Nicolas Kaufman, J.R. Patterson, A. Rinkevicius, A. Ryd, L. Skinnari, L. Soffi, W. Sun, S.M. Tan, W.D. Teo, J. Thom, J. Thompson, J. Tucker, Y. Weng, P. Wittich

Fermi National Accelerator Laboratory, Batavia, USA
S. Abdullin, M. Albrow, G. Apollinari, S. Banerjee, L.A.T. Bauerdick, A. Beretvas, J. Berryhill, P.C. Bhat, G. Bolla, K. Burkett, J.N. Butler, H.W.K. Cheung, F. Chlebana, S. Cihangir, V.D. Elvira, I. Fisk, J. Freeman, E. Gottschalk, L. Gray, D. Green, S. Grünendahl, O. Gutsche, J. Hanlon, D. Hare, R.M. Harris, S. Hasegawa, J. Hirschauer, Z. Hu, B. Jayatilaka, S. Jindariani, M. Johnson, U. Joshi, B. Klima, B. Kreis, S. Lammel, J. Lewis, J. Linacre, D. Lincoln, R. Lipton, T. Liu, R. Lopes De Sá, J. Lykken, K. Maeshima, J.M. Marraffino, S. Maruyama, D. Mason, P. McBride, P. Merkel, S. Mrenna, S. Nahn, C. Newman-Holmes[†], V. O'Dell, K. Pedro, O. Prokofyev,

G. Rakness, E. Sexton-Kennedy, A. Soha, W.J. Spalding, L. Spiegel, S. Stoynev, N. Strobbe, L. Taylor, S. Tkaczyk, N.V. Tran, L. Uplegger, E.W. Vaandering, C. Vernieri, M. Verzocchi, R. Vidal, M. Wang, H.A. Weber, A. Whitbeck

University of Florida, Gainesville, USA
D. Acosta, P. Avery, P. Bortignon, D. Bourilkov, A. Brinkerhoff, A. Carnes, M. Carver, D. Curry, S. Das, R.D. Field, I.K. Furic, J. Konigsberg, A. Korytov, K. Kotov, P. Ma, K. Matchev, H. Mei, P. Milenovic[64], G. Mitselmakher, D. Rank, R. Rossin, L. Shchutska, M. Snowball, D. Sperka, N. Terentyev, L. Thomas, J. Wang, S. Wang, J. Yelton

Florida International University, Miami, USA
S. Hewamanage, S. Linn, P. Markowitz, G. Martinez, J.L. Rodriguez

Florida State University, Tallahassee, USA
A. Ackert, J.R. Adams, T. Adams, A. Askew, S. Bein, J. Bochenek, B. Diamond, J. Haas, S. Hagopian, V. Hagopian, K.F. Johnson, A. Khatiwada, H. Prosper, M. Weinberg

Florida Institute of Technology, Melbourne, USA
M.M. Baarmand, V. Bhopatkar, S. Colafranceschi[65], M. Hohlmann, H. Kalakhety, D. Noonan, T. Roy, F. Yumiceva

University of Illinois at Chicago (UIC), Chicago, USA
M.R. Adams, L. Apanasevich, D. Berry, R.R. Betts, I. Bucinskaite, R. Cavanaugh, O. Evdokimov, L. Gauthier, C.E. Gerber, D.J. Hofman, P. Kurt, C. O'Brien, I.D. Sandoval Gonzalez, P. Turner, N. Varelas, Z. Wu, M. Zakaria, J. Zhang

The University of Iowa, Iowa City, USA
B. Bilki[66], W. Clarida, K. Dilsiz, S. Durgut, R.P. Gandrajula, M. Haytmyradov, V. Khristenko, J.-P. Merlo, H. Mermerkaya[67], A. Mestvirishvili, A. Moeller, J. Nachtman, H. Ogul, Y. Onel, F. Ozok[68], A. Penzo, C. Snyder, E. Tiras, J. Wetzel, K. Yi

Johns Hopkins University, Baltimore, USA
I. Anderson, B.A. Barnett, B. Blumenfeld, A. Cocoros, N. Eminizer, D. Fehling, L. Feng, A.V. Gritsan, P. Maksimovic, M. Osherson, J. Roskes, U. Sarica, M. Swartz, M. Xiao, Y. Xin, C. You

The University of Kansas, Lawrence, USA
P. Baringer, A. Bean, C. Bruner, R.P. Kenny III, D. Majumder, M. Malek, W. Mcbrayer, M. Murray, S. Sanders, R. Stringer, Q. Wang

Kansas State University, Manhattan, USA
A. Ivanov, K. Kaadze, S. Khalil, M. Makouski, Y. Maravin, A. Mohammadi, L.K. Saini, N. Skhirtladze, S. Toda

Lawrence Livermore National Laboratory, Livermore, USA
D. Lange, F. Rebassoo, D. Wright

University of Maryland, College Park, USA
C. Anelli, A. Baden, O. Baron, A. Belloni, B. Calvert, S.C. Eno, C. Ferraioli, J.A. Gomez, N.J. Hadley, S. Jabeen, R.G. Kellogg, T. Kolberg, J. Kunkle, Y. Lu, A.C. Mignerey, Y.H. Shin, A. Skuja, M.B. Tonjes, S.C. Tonwar

Massachusetts Institute of Technology, Cambridge, USA
A. Apyan, R. Barbieri, A. Baty, R. Bi, K. Bierwagen, S. Brandt, W. Busza, I.A. Cali, Z. Demiragli, L. Di Matteo, G. Gomez Ceballos, M. Goncharov, D. Gulhan, Y. Iiyama, G.M. Innocenti,

M. Klute, D. Kovalskyi, Y.S. Lai, Y.-J. Lee, A. Levin, P.D. Luckey, A.C. Marini, C. Mcginn, C. Mironov, S. Narayanan, X. Niu, C. Paus, C. Roland, G. Roland, J. Salfeld-Nebgen, G.S.F. Stephans, K. Sumorok, K. Tatar, M. Varma, D. Velicanu, J. Veverka, J. Wang, T.W. Wang, B. Wyslouch, M. Yang, V. Zhukova

University of Minnesota, Minneapolis, USA
A.C. Benvenuti, B. Dahmes, A. Evans, A. Finkel, A. Gude, P. Hansen, S. Kalafut, S.C. Kao, K. Klapoetke, Y. Kubota, Z. Lesko, J. Mans, S. Nourbakhsh, N. Ruckstuhl, R. Rusack, N. Tambe, J. Turkewitz

University of Mississippi, Oxford, USA
J.G. Acosta, S. Oliveros

University of Nebraska-Lincoln, Lincoln, USA
E. Avdeeva, R. Bartek, K. Bloom, S. Bose, D.R. Claes, A. Dominguez, C. Fangmeier, R. Gonzalez Suarez, R. Kamalieddin, D. Knowlton, I. Kravchenko, F. Meier, J. Monroy, F. Ratnikov, J.E. Siado, G.R. Snow

State University of New York at Buffalo, Buffalo, USA
M. Alyari, J. Dolen, J. George, A. Godshalk, C. Harrington, I. Iashvili, J. Kaisen, A. Kharchilava, A. Kumar, S. Rappoccio, B. Roozbahani

Northeastern University, Boston, USA
G. Alverson, E. Barberis, D. Baumgartel, M. Chasco, A. Hortiangtham, A. Massironi, D.M. Morse, D. Nash, T. Orimoto, R. Teixeira De Lima, D. Trocino, R.-J. Wang, D. Wood, J. Zhang

Northwestern University, Evanston, USA
S. Bhattacharya, K.A. Hahn, A. Kubik, J.F. Low, N. Mucia, N. Odell, B. Pollack, M. Schmitt, K. Sung, M. Trovato, M. Velasco

University of Notre Dame, Notre Dame, USA
N. Dev, M. Hildreth, C. Jessop, D.J. Karmgard, N. Kellams, K. Lannon, N. Marinelli, F. Meng, C. Mueller, Y. Musienko[37], M. Planer, A. Reinsvold, R. Ruchti, G. Smith, S. Taroni, N. Valls, M. Wayne, M. Wolf, A. Woodard

The Ohio State University, Columbus, USA
L. Antonelli, J. Brinson, B. Bylsma, L.S. Durkin, S. Flowers, A. Hart, C. Hill, R. Hughes, W. Ji, T.Y. Ling, B. Liu, W. Luo, D. Puigh, M. Rodenburg, B.L. Winer, H.W. Wulsin

Princeton University, Princeton, USA
O. Driga, P. Elmer, J. Hardenbrook, P. Hebda, S.A. Koay, P. Lujan, D. Marlow, T. Medvedeva, M. Mooney, J. Olsen, C. Palmer, P. Piroué, D. Stickland, C. Tully, A. Zuranski

University of Puerto Rico, Mayaguez, USA
S. Malik

Purdue University, West Lafayette, USA
A. Barker, V.E. Barnes, D. Benedetti, D. Bortoletto, L. Gutay, M.K. Jha, M. Jones, A.W. Jung, K. Jung, A. Kumar, D.H. Miller, N. Neumeister, B.C. Radburn-Smith, X. Shi, I. Shipsey, D. Silvers, J. Sun, A. Svyatkovskiy, F. Wang, W. Xie, L. Xu

Purdue University Calumet, Hammond, USA
N. Parashar, J. Stupak

Rice University, Houston, USA
A. Adair, B. Akgun, Z. Chen, K.M. Ecklund, F.J.M. Geurts, M. Guilbaud, W. Li, B. Michlin, M. Northup, B.P. Padley, R. Redjimi, J. Roberts, J. Rorie, Z. Tu, J. Zabel

University of Rochester, Rochester, USA
B. Betchart, A. Bodek, P. de Barbaro, R. Demina, Y. Eshaq, T. Ferbel, M. Galanti, A. Garcia-Bellido, J. Han, O. Hindrichs, A. Khukhunaishvili, K.H. Lo, P. Tan, M. Verzetti

Rutgers, The State University of New Jersey, Piscataway, USA
J.P. Chou, E. Contreras-Campana, D. Ferencek, Y. Gershtein, E. Halkiadakis, M. Heindl, D. Hidas, E. Hughes, S. Kaplan, R. Kunnawalkam Elayavalli, A. Lath, K. Nash, H. Saka, S. Salur, S. Schnetzer, D. Sheffield, S. Somalwar, R. Stone, S. Thomas, P. Thomassen, M. Walker

University of Tennessee, Knoxville, USA
M. Foerster, G. Riley, K. Rose, S. Spanier, K. Thapa

Texas A&M University, College Station, USA
O. Bouhali[69], A. Castaneda Hernandez[69], A. Celik, M. Dalchenko, M. De Mattia, A. Delgado, S. Dildick, R. Eusebi, J. Gilmore, T. Huang, T. Kamon[70], V. Krutelyov, R. Mueller, I. Osipenkov, Y. Pakhotin, R. Patel, A. Perloff, A. Rose, A. Safonov, A. Tatarinov, K.A. Ulmer[2]

Texas Tech University, Lubbock, USA
N. Akchurin, C. Cowden, J. Damgov, C. Dragoiu, P.R. Dudero, J. Faulkner, S. Kunori, K. Lamichhane, S.W. Lee, T. Libeiro, S. Undleeb, I. Volobouev

Vanderbilt University, Nashville, USA
E. Appelt, A.G. Delannoy, S. Greene, A. Gurrola, R. Janjam, W. Johns, C. Maguire, Y. Mao, A. Melo, H. Ni, P. Sheldon, S. Tuo, J. Velkovska, Q. Xu

University of Virginia, Charlottesville, USA
M.W. Arenton, B. Cox, B. Francis, J. Goodell, R. Hirosky, A. Ledovskoy, H. Li, C. Lin, C. Neu, T. Sinthuprasith, X. Sun, Y. Wang, E. Wolfe, J. Wood, F. Xia

Wayne State University, Detroit, USA
C. Clarke, R. Harr, P.E. Karchin, C. Kottachchi Kankanamge Don, P. Lamichhane, J. Sturdy

University of Wisconsin - Madison, Madison, WI, USA
D.A. Belknap, D. Carlsmith, S. Dasu, L. Dodd, S. Duric, B. Gomber, M. Grothe, M. Herndon, A. Hervé, P. Klabbers, A. Lanaro, A. Levine, K. Long, R. Loveless, A. Mohapatra, I. Ojalvo, T. Perry, G.A. Pierro, G. Polese, T. Ruggles, T. Sarangi, A. Savin, A. Sharma, N. Smith, W.H. Smith, D. Taylor, P. Verwilligen, N. Woods

†: Deceased
1: Also at Vienna University of Technology, Vienna, Austria
2: Also at CERN, European Organization for Nuclear Research, Geneva, Switzerland
3: Also at State Key Laboratory of Nuclear Physics and Technology, Peking University, Beijing, China
4: Also at Institut Pluridisciplinaire Hubert Curien, Université de Strasbourg, Université de Haute Alsace Mulhouse, CNRS/IN2P3, Strasbourg, France
5: Also at Skobeltsyn Institute of Nuclear Physics, Lomonosov Moscow State University, Moscow, Russia
6: Also at Universidade Estadual de Campinas, Campinas, Brazil
7: Also at Centre National de la Recherche Scientifique (CNRS) - IN2P3, Paris, France
8: Also at Laboratoire Leprince-Ringuet, Ecole Polytechnique, IN2P3-CNRS, Palaiseau, France

9: Also at Joint Institute for Nuclear Research, Dubna, Russia
10: Also at British University in Egypt, Cairo, Egypt
11: Now at Suez University, Suez, Egypt
12: Also at Cairo University, Cairo, Egypt
13: Also at Fayoum University, El-Fayoum, Egypt
14: Also at Université de Haute Alsace, Mulhouse, France
15: Also at Tbilisi State University, Tbilisi, Georgia
16: Also at RWTH Aachen University, III. Physikalisches Institut A, Aachen, Germany
17: Also at University of Hamburg, Hamburg, Germany
18: Also at Brandenburg University of Technology, Cottbus, Germany
19: Also at Institute of Nuclear Research ATOMKI, Debrecen, Hungary
20: Also at Eötvös Loránd University, Budapest, Hungary
21: Also at University of Debrecen, Debrecen, Hungary
22: Also at Wigner Research Centre for Physics, Budapest, Hungary
23: Also at Indian Institute of Science Education and Research, Bhopal, India
24: Also at University of Visva-Bharati, Santiniketan, India
25: Now at King Abdulaziz University, Jeddah, Saudi Arabia
26: Also at University of Ruhuna, Matara, Sri Lanka
27: Also at Isfahan University of Technology, Isfahan, Iran
28: Also at University of Tehran, Department of Engineering Science, Tehran, Iran
29: Also at Plasma Physics Research Center, Science and Research Branch, Islamic Azad University, Tehran, Iran
30: Also at Laboratori Nazionali di Legnaro dell'INFN, Legnaro, Italy
31: Also at Università degli Studi di Siena, Siena, Italy
32: Also at Purdue University, West Lafayette, USA
33: Also at International Islamic University of Malaysia, Kuala Lumpur, Malaysia
34: Also at Malaysian Nuclear Agency, MOSTI, Kajang, Malaysia
35: Also at Consejo Nacional de Ciencia y Tecnología, Mexico city, Mexico
36: Also at Warsaw University of Technology, Institute of Electronic Systems, Warsaw, Poland
37: Also at Institute for Nuclear Research, Moscow, Russia
38: Now at National Research Nuclear University 'Moscow Engineering Physics Institute' (MEPhI), Moscow, Russia
39: Also at St. Petersburg State Polytechnical University, St. Petersburg, Russia
40: Also at California Institute of Technology, Pasadena, USA
41: Also at Faculty of Physics, University of Belgrade, Belgrade, Serbia
42: Also at INFN Sezione di Roma; Università di Roma, Roma, Italy
43: Also at National Technical University of Athens, Athens, Greece
44: Also at Scuola Normale e Sezione dell'INFN, Pisa, Italy
45: Also at National and Kapodistrian University of Athens, Athens, Greece
46: Also at Institute for Theoretical and Experimental Physics, Moscow, Russia
47: Also at Albert Einstein Center for Fundamental Physics, Bern, Switzerland
48: Also at Adiyaman University, Adiyaman, Turkey
49: Also at Mersin University, Mersin, Turkey
50: Also at Cag University, Mersin, Turkey
51: Also at Piri Reis University, Istanbul, Turkey
52: Also at Gaziosmanpasa University, Tokat, Turkey
53: Also at Ozyegin University, Istanbul, Turkey
54: Also at Izmir Institute of Technology, Izmir, Turkey
55: Also at Marmara University, Istanbul, Turkey

56: Also at Kafkas University, Kars, Turkey
57: Also at Istanbul Bilgi University, Istanbul, Turkey
58: Also at Yildiz Technical University, Istanbul, Turkey
59: Also at Hacettepe University, Ankara, Turkey
60: Also at Rutherford Appleton Laboratory, Didcot, United Kingdom
61: Also at School of Physics and Astronomy, University of Southampton, Southampton, United Kingdom
62: Also at Instituto de Astrofísica de Canarias, La Laguna, Spain
63: Also at Utah Valley University, Orem, USA
64: Also at University of Belgrade, Faculty of Physics and Vinca Institute of Nuclear Sciences, Belgrade, Serbia
65: Also at Facoltà Ingegneria, Università di Roma, Roma, Italy
66: Also at Argonne National Laboratory, Argonne, USA
67: Also at Erzincan University, Erzincan, Turkey
68: Also at Mimar Sinan University, Istanbul, Istanbul, Turkey
69: Also at Texas A&M University at Qatar, Doha, Qatar
70: Also at Kyungpook National University, Daegu, Korea